C.3

LAMS-2882

# LOS ALAMOS SCIENTIFIC LABORATORY
## OF THE UNIVERSITY OF CALIFORNIA ○ LOS ALAMOS    NEW MEXICO

SOME APPROXIMATE CALCULATIONS OF
THE WALL PRESSURE PROFILE FOR THE CASE
OF A CHAPMAN-JOUQUET DETONATION IN A FINITE MASS
OF HIGH EXPLOSIVE ADJACENT TO A RIGID WALL

# LOS ALAMOS SCIENTIFIC LABORATORY
## OF THE UNIVERSITY OF CALIFORNIA    LOS ALAMOS    NEW MEXICO

SOME APPROXIMATE CALCULATIONS OF

THE WALL PRESSURE PROFILE FOR THE CASE

OF A CHAPMAN-JOUQUET DETONATION IN A FINITE MASS

OF HIGH EXPLOSIVE ADJACENT TO A RIGID WALL

by

Kenneth A. Meyer
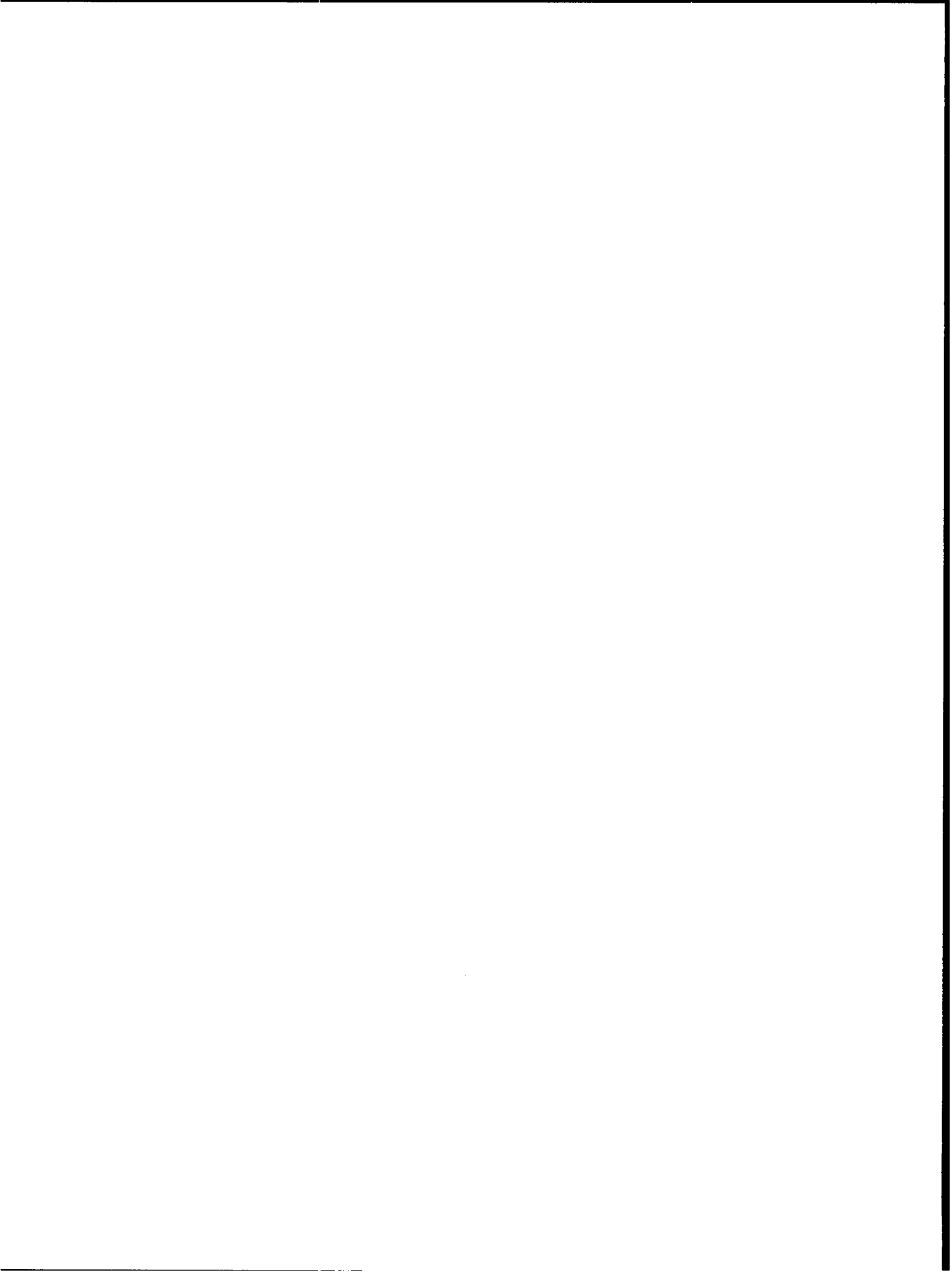
## ABSTRACT

This paper considers the problem of the detonation of a slab of high explosive adjacent to a rigid wall with a vacuum as the other boundary. The reflected shock is computed using Whitham's approximation. The pressure profile at the wall is computed by various approximate methods and results are compared with those obtained from a numerical solution using a Lagrangian code.
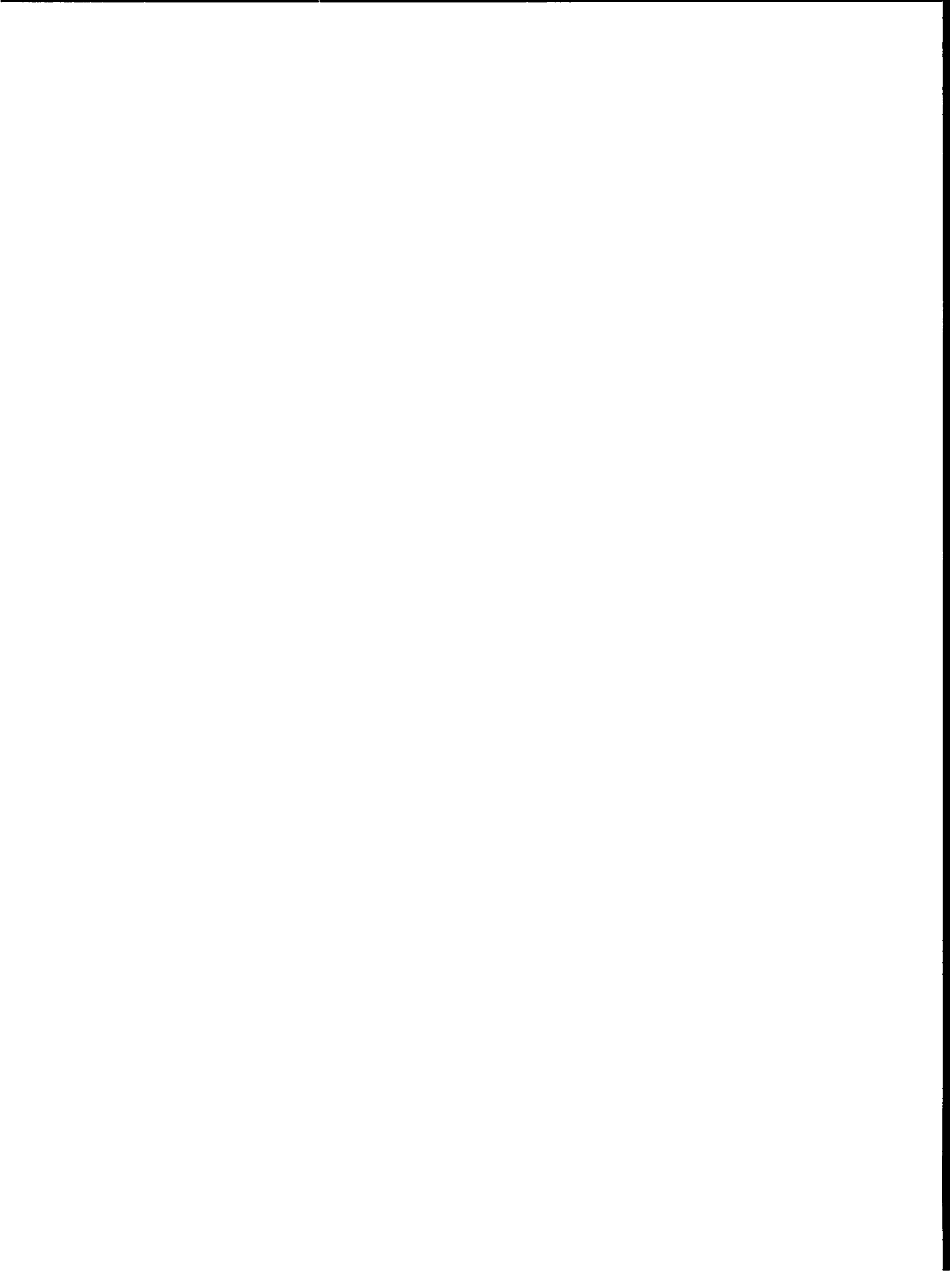
# 1. INTRODUCTION

The problem studied is that of a slab of high explosive with a
rigid wall as one boundary and a vacuum as the other (Figures 1 and 2),
with the high explosive being detonated at the vacuum boundary. The
problem is one dimensional with the high explosive and the wall continu-
ing to infinity in the y and z direction. The reflection of the deton-
ation at the rigid wall and an approximation of the flow between the
reflected shock and rigid wall is investigated. Reflected shock paths
are computed for various values of the adiabatic exponent $\gamma$. Wall
pressures behind the reflected shock are computed for $\gamma = 3$ and $\gamma = 1.4$.

The flow can be considered as consisting of three regions (Figure 2):

> Region I    Unexploded high explosive,
>
> Region II   Simple wave expansion of the detonation products
> (isentropic),
>
> Region III  Region between reflected shock and wall, assumed
> to be isentropic in the region of interest.

The detonation is computed using the conservation laws and the
assumption of a Chapman-Jouquet detonation, $c = |u-D|$, where c is the
sound speed behind the detonation, u is the gas velocity behind the
detonation, and D is the detonation velocity.

5
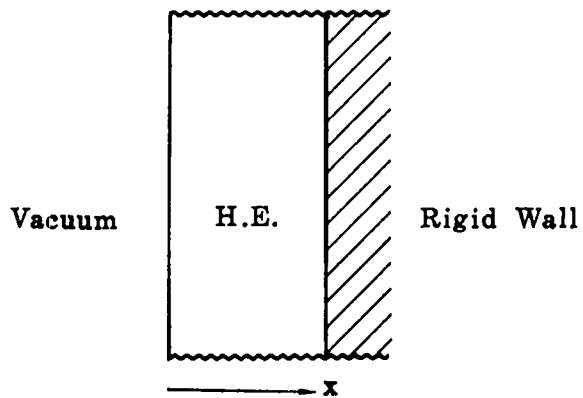
Figure 1.   Initial Configuration of System
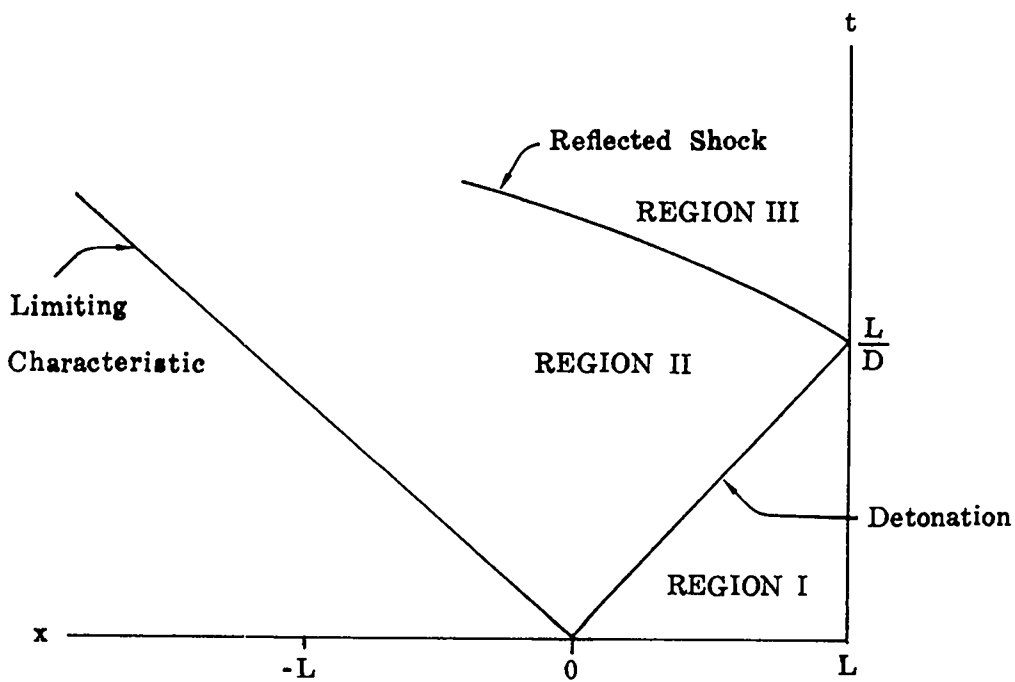


Figure 2.   Typical x-t Plot Showing Detonation and Subsequent Flow

Region II is then a simple wave region adjacent to a line of constant state, i.e., the detonation, and extending to the limiting characteristic separating the flow and the vacuum.

The reflected shock is computed by a method given by Whitham (ref.1) which applies the characteristic relation $dp + \rho c\,du = 0$ (or $dp - \rho c\,du = 0$ depending on the direction of the shock) to the flow quantities at the shock. The quantities in the above equation are known in terms of the shock Mach number M from the Rankine-Hugoniot shock relations, hence an equation for the variation of the shock strength can be obtained by substituting the shock relations into the appropriate characteristic relation. The solution of this differential equation enables one to obtain the shock path and values of $p$, $\rho$, $c$, $u$ behind the shock as functions of the shock path. The Whitham shock paths are also compared with results obtained from a numerical solution to the complete problem.

The flow behind the shock is considered to be isentropic in the region of interest. The Riemann invariants r and s $\left( r = \dfrac{u}{2} + \dfrac{c}{\gamma-1}, \right.$ $\left. -s = \dfrac{u}{2} - \dfrac{c}{\gamma-1} \right)$ on the shock can be related by $s = s_0 + \alpha r$, with $s_0$ and $\alpha$ obtained from the shock solution. The error introduced in s is less than one percent. Calculations were made using the above relation and the simpler expression $s = s_0$, i.e., the shock represented by a characteristic. Since the flow is assumed to be isentropic, it is possible to transform to the speedgraph plane (see for example ref.2, pp. 160-171) with u and c as independent variables. By representing t on the shock as a quadratic in r (2 percent maximum error), it is possible to obtain an analytic

7

solution in the region between the shock and the wall. It should be noted that the shock is a timelike curve (see, for example, ref.3, p.57); and therefore in x,t space either u or c, but not both, may be specified, although both are obtained from the Whitham solution. In the transformed variables the shock is represented by a curve u = u(c) and t is specified as t = t(c) on this curve. The solution includes x = x[c,u(c)] for the shock curve as a consequence of its timelike character. The solution in Region II then actually has this newly determined "shock" as its boundary.

For $\gamma = 3$ other approximations were considered and will be mentioned in the text.

The results of this investigation indicate that the wall pressure vs. time curve is quite insensitive to the type of approximation made; and it would appear that using the simplest assumption for $\gamma = 3$, that of ignoring the reflected shock and continuing the straight characteristics of the original expansion to the wall to obtain the pressure, is quite adequate for approximate calculations. Going one step further one would suspect that using this approximation for propelling a rigid mass would be equally valid.

## 2. EQUATIONS

### A. Detonation Front

The equations of the detonation are obtained from the conservation laws

Mass $\qquad \rho_0(u_0 - D) = \rho_1(u_1 - D) \qquad\qquad$ (1)

Momentum $\qquad p_0 + \rho_0(u_1 - D)^2 = p_1 + \rho_1(u_1 - D)^2 \qquad\qquad$ (2)

Energy $\qquad E_0(p_0, \rho_0) + \dfrac{p_0}{\rho_0} + \dfrac{1}{2}(u_0 - D)^2 = E_1(p_1, \rho_1) + \dfrac{p_1}{\rho_1} + \dfrac{1}{2}(u_1 - D)^2$

$\qquad\qquad\qquad\qquad\qquad\qquad\qquad\qquad\qquad\qquad\qquad\qquad$ (3)

where the subscript (0) applies to the unburned explosive and the sub-script (1) applies to the detonation products.

For a forward facing Chapman-Jouquet detonation $D = u_1 + c_1$. It will be assumed that the detonation proceeds into a stationary explosive, $u_0 = 0$, and for simplicity that $p_0 = 0$. The energy of the unburned explosive $E_0$ will be represented by $e_0(p_0, \rho_0) + Q$ where $Q$ is the chemical energy. Since $e_0$ is small compared to $Q$ it will be ignored. With the above assumptions the conservation laws become

$$\rho_0 D = \rho_1(D - u_1) \qquad\qquad (1a)$$

$$\rho_0 D^2 = p_1 + \rho_1(D - u_1)^2 \qquad\qquad (2a)$$

$$\frac{1}{2}D^2 + Q = \frac{\gamma}{\gamma - 1}\frac{p_1}{\rho_1} + \frac{1}{2}(u_1 - D)^2 \qquad\qquad (3a)$$

where in Equation (3a) use has been made of the relations

9

$$c_1^2 = \frac{\gamma p_1}{\rho_1} \ , \ E_1 = e_1 = \frac{1}{\gamma-1} \frac{p_1}{\rho_1} \tag{4}$$

for the detonation products.

Combining these equations one obtains the following for the flow immediately behind the detonation:

$$c_1 = \frac{\gamma}{\gamma+1} D \tag{5}$$

$$u_1 = \frac{1}{\gamma+1} D \tag{6}$$

$$\rho_1 = \frac{\gamma+1}{\gamma} \rho_0 \tag{7}$$

$$p_1 = \frac{1}{\gamma+1} \rho_0 D^2 \tag{8}$$

$$D = \sqrt{2(\gamma^2-1)Q} \ . \tag{9}$$

B.    Region II

The region behind the detonation is a simple wave region in which the following characteristic equations hold:

$$\frac{dx}{dt} = u + c \tag{10}$$

$$\left.\begin{array}{l}\\ \\ \\ \\ \\ \\ \\ \end{array}\right\} \text{On } c^+$$

$$\frac{u}{2} + \frac{c}{\gamma-1} = r \tag{11}$$

10

$$\frac{dx}{dt} = u - c \qquad\qquad (12)$$

$$\left. \phantom{x} \right\} \text{ On } C^-$$

$$\frac{u}{2} - \frac{c}{\gamma-1} = -s. \qquad\qquad (13)$$

For a Chapman-Jouquet detonation $D = u_1 + c_1$, hence the detonation front is coincident with the leading $C^+$ characteristic. The slope of this characteristic and the values of u, c, etc. it carries can be obtained from Equations (5) through (8). With the coordinates as shown in Figure 2 the equation of the $C^+$ characteristic and the expression for the corresponding Riemann invariant are, respectively,

$$\frac{x}{t} = u + c \qquad\qquad (14)$$

$$\frac{u}{2} + \frac{c}{\gamma-1} = r(\frac{x}{t}). \qquad\qquad (15)$$

Since all $C^-$ characteristics originate at the detonation where Equations (5) through (8) hold, we have from (13),

$$-s = \frac{u}{2} - \frac{c}{\gamma-1} = \frac{-D}{2(\gamma-1)}. \qquad\qquad (16)$$

Combining Equations (14) through (16) the following are obtained:

$$r = \frac{2}{\gamma+1} \frac{x}{t} + \frac{3-\gamma}{2(\gamma^2-1)} D \qquad\qquad (17)$$

11

$$u = \frac{2}{\gamma+1}\frac{x}{t} - \frac{D}{\gamma+1} \tag{18}$$

$$c = \frac{\gamma-1}{\gamma+1}\frac{x}{t} + \frac{D}{\gamma+1}. \tag{19}$$

We now have the equations of the $C^+$ characteristics and expressions for $u(x,t)$, $c(x,t)$, $r(x,t)$ and $s = s_0$. All that remains is to determine the equation of the $C^-$ characteristics. Substituting for $u$ and $c$ from Equations (18) and (19) into Equation (12) yields for the $C^-$ characteristic

$$\frac{dx}{dt} = \frac{3-\gamma}{\gamma+1}\frac{x}{t} - \frac{2D}{\gamma+1}$$

which integrates to

$$(x + \frac{D}{\gamma-1}t) = (x_0 + \frac{D}{\gamma-1}t_0)(\frac{t}{t_0})^{3-\gamma/\gamma+1} \tag{20}$$

where $x_0$ and $t_0$ refer to the intersection of the characteristic with the detonation.

The equations will be put in dimensionless form using the following definitions:

$$\bar{x} = \frac{x}{L}, \quad \bar{t} = \frac{Dt}{L}, \quad \bar{u} = \frac{u}{D}, \quad \bar{c} = \frac{c}{D}, \quad \bar{r} = \frac{r}{D}, \quad \text{and } \bar{\eta} = \frac{\bar{x}}{\bar{t}}.$$

The preceding equations then become

12

$$\bar{x} = \frac{-1}{\gamma-1}\,\bar{t} + \frac{\gamma}{\gamma-1}\,\bar{t}_0^{\,2(\gamma-1/\gamma+1)}\,\bar{t}^{(3-\gamma/\gamma-1)} \left.\vphantom{\begin{array}{c}a\\a\\a\end{array}}\right\} \quad\quad\quad\text{(20a)}$$

$$\qquad\qquad\qquad\qquad\qquad\qquad\qquad\qquad\qquad\quad c^{-}$$

$$\frac{\bar{u}}{2} - \frac{\bar{c}}{\gamma-1} = -\frac{1}{2(\gamma-1)} \qquad\qquad\qquad\qquad\text{(16a)}$$

$$\bar{\eta} = \bar{u} + \bar{c} \left.\vphantom{\begin{array}{c}a\\a\\a\end{array}}\right\} \qquad\qquad\qquad\qquad\qquad\text{(14a)}$$

$$\qquad\qquad\qquad\qquad\qquad\qquad\qquad\qquad\qquad\quad c^{+}$$

$$r = \frac{2}{\gamma+1}\,\bar{\eta} + \frac{3-\gamma}{2(\gamma^2-1)} \qquad\qquad\qquad\text{(17a)}$$

$$u = \frac{2}{\gamma+1}\left(\bar{\eta} - \frac{1}{2}\right) \qquad\qquad\qquad\qquad\text{(18a)}$$

$$\bar{c} = \frac{\gamma-1}{\gamma+1}\left(\bar{\eta} + \frac{1}{\gamma-1}\right). \qquad\qquad\qquad\text{(19a)}$$

Using the polytropic relations

$$\left(\frac{\rho}{\rho_0}\right)^{\gamma-1} = \left(\frac{c}{c_0}\right)^2, \quad p = p_0\left(\frac{\rho}{\rho_0}\right)^{\gamma} \qquad\qquad\text{(21)}$$

where $p_0$, $\rho_0$, and $c_0$ are reference quantities, the following are obtained from Equation (19a):

$$\rho = \frac{\rho_0}{c_0^{\,2/\gamma-1}}\left[\frac{\gamma-1}{\gamma+1}\left(\bar{\eta} + \frac{1}{\gamma-1}\right)\right]^{2/\gamma-1} \qquad\qquad\text{(22)}$$

$$p = \frac{p_0}{c_0^{\,2\gamma/\gamma-1}}\left[\frac{\gamma-1}{\gamma+1}\left(\bar{\eta} + \frac{1}{\gamma-1}\right)\right]^{2\gamma/\gamma-1}. \qquad\qquad\text{(23)}$$

13

It will be convenient at this time to form the differentials of the quantities in Equations (18a), (19a), (22), and (23) for later use.

$$d\bar{u} = \frac{2}{\gamma+1} d\bar{\eta} \tag{24}$$

$$d\bar{c} = \frac{\gamma-1}{\gamma+1} d\bar{\eta} \tag{25}$$

$$d\rho_1 = \frac{2}{\gamma+1} \frac{\rho_0}{c_0^{2/\gamma-1}} \left[\frac{\gamma-1}{\gamma+1}\left(\bar{\eta} + \frac{1}{\gamma-1}\right)\right]^{3-\gamma/\gamma-1} d\bar{\eta} \tag{26}$$

$$dp_1 = \frac{2\gamma}{\gamma+1} \frac{p_0}{c_0^{2\gamma/\gamma-1}} \left[\frac{\gamma-1}{\gamma+1}\left(\bar{\eta} + \frac{1}{\gamma-1}\right)\right]^{\gamma+1/\gamma-1} d\bar{\eta} \tag{27}$$

C.   Shock Equations

The Rankine-Hugoniot shock relations may be written as follows (see for example ref.4, p.120):

$$\bar{u}_s = \bar{u} + \frac{2}{\gamma+1} \bar{c}M\left(1 - \frac{1}{M^2}\right) \tag{28}$$

$$\bar{c}_s = \frac{\bar{c}}{M} \left[1 + \frac{2\gamma}{\gamma+1}(M^2-1)\right]^{1/2}\left[1 + \frac{\gamma-1}{\gamma+1}(M^2-1)\right]^{1/2} \tag{29}$$

$$p_s = p\left[1 + \frac{2\gamma}{\gamma+1}(M^2-1)\right] \tag{30}$$

$$\rho_s = \frac{\rho M^2}{\left[1 + \frac{\gamma-1}{\gamma+1}(M^2-1)\right]} \tag{31}$$

where the subscript s refers to the flow behind the shock and the

14

unsubscripted quantities are in front of the shock. The Mach number M
is defined as

$$M = \frac{\bar{U} - \bar{u}}{\bar{c}} \tag{32}$$

where $\bar{U} = U/D$, U being the shock velocity. Note that the Mach number
carries the same sign as $\bar{U} - \bar{u}$.

The procedure described by Whitham (ref. 1) for computing the shock
path requires that the flow variables at the shock wave satisfy

$$dp_s - \rho_s c_s \, du_s = 0 \text{ (for a left moving shock).} \tag{33}$$

Differentiating Equations (28) and (30) we have

$$d\bar{u}_s = d\bar{u} + \frac{2}{\gamma+1} M\left(1 - \frac{1}{M^2}\right)d\bar{c} + \frac{2}{\gamma+1} \bar{c}\left(1 + \frac{1}{M^2}\right)dM \tag{34}$$

$$dp_s = \left[1 + \frac{2\gamma}{\gamma+1}(M^2-1)\right]dp + p\left(\frac{4\gamma}{\gamma+1}\right)M dM. \tag{35}$$

Substituting Equations (29), (31), (34), and (35) into (33) gives
the following result:

$$\left[1 + \frac{2\gamma}{\gamma+1}(M^2-1)\right]dp + p\left(\frac{4\gamma}{\gamma+1}\right)MdM$$

$$-\left\{\rho\bar{c}M\,\frac{[1 + \frac{2\gamma}{\gamma+1}(M^2-1)]^{1/2}}{[1 + \frac{\gamma-1}{\gamma+1}(M^2-1)]^{1/2}}\left[d\bar{u} + \frac{2}{\gamma+1}M\left(1 - \frac{1}{M^2}\right)d\bar{c}\right.\right.$$

$$\left.\left.+\frac{2}{\gamma+1}\bar{c}\left(1 + \frac{1}{M^2}\right)dM\right]\right\} = 0. \tag{36}$$

Replacing $\rho$, $\bar{c}$, etc., in Equation (36) by Equations (18a), (19a), and (22) through (27) one obtains, after algebraic manipulation, the following differential equation in M and $\bar{\eta}$:

$$\frac{dM}{d\bar{\eta}} = -\frac{\frac{2}{\gamma-1}\left[\gamma M^2 - \frac{\gamma-1}{2}\right] - \left[M - \frac{1}{M} + \frac{\gamma+1}{\gamma-1}\right]\left[\left(\gamma M^2 - \frac{\gamma-1}{2}\right)\left(\frac{M^2}{(\gamma-1/2)M^2+1}\right)\right]^{1/2}}{\left(\eta + \frac{1}{\gamma-1}\right)\left\{2M - \left(\frac{M^2+1}{M^2}\right)\left[\gamma M^2 - \frac{\gamma-1}{2}\left(\frac{M^2}{(\gamma-1/2)M^2+1}\right)\right]^{1/2}\right\}} . \tag{37}$$

This equation can be integrated numerically to give $M = M(\bar{\eta})$, the integration to be carried out between $-1/2 \leq \bar{\eta} \leq 1$. The initial condition on $M(\bar{\eta})$ is obtained from the reflection of the detonation.

From the conservation laws

$$\frac{\bar{u}_2 - \bar{u}_1}{\bar{c}_1} = \frac{2}{\gamma+1}\left(M_1 - \frac{1}{M_1}\right).$$

At the instant of reflection

16

$$\bar{u}_2 = 0$$

$$\bar{u}_1 = \frac{1}{\gamma+1}$$

$$\bar{c}_1 = \frac{\gamma}{\gamma+1}$$

giving

$$M_1(1) = \frac{\gamma+1}{4\gamma}\left[1 + \sqrt{1 + (\frac{4\gamma}{\gamma+1})^2}\right].\tag{38}$$

Knowing $M = M(\bar{\eta})$ the shock velocity is obtained from Equation (32) as

$$\bar{U} = M\bar{c} + \bar{u} = M(\bar{\eta})\left(\frac{\gamma-1}{\gamma+1}\right)\left(\bar{\eta} + \frac{1}{\gamma-1}\right) + \frac{2}{\gamma+1}(\bar{\eta} - \frac{1}{2}).\tag{39}$$

This equation can also be written as

$$\frac{d\bar{x}_s}{d\bar{t}} = \bar{u}\left(\frac{\bar{x}_s}{\bar{t}}\right)\tag{40}$$

where $\bar{x}_s$ is the coordinate of the shock. Integrating from $\bar{x}_s(1) = 1$ gives the equation of the shock path $\bar{x}_s = \bar{x}_s(\bar{t})$.

D. Region III

In obtaining a solution for Region III it is assumed that the flow behind the shock can be considered isentropic in the region of interest.

The equations of motion governing the one-dimensional non-steady flow of an inviscid elastic fluid can be written as

Continuity
$$\bar{\rho}\,\frac{\partial \bar{u}}{\partial \bar{x}} + \bar{u}\,\frac{\partial \bar{\rho}}{\partial \bar{x}} + \frac{\partial \bar{\rho}}{\partial \bar{t}} = 0 \qquad (41)$$

Momentum
$$\bar{u}\,\frac{\partial \bar{u}}{\partial \bar{x}} + \frac{\bar{c}^{-2}}{\bar{\rho}}\,\frac{\partial \bar{\rho}}{\partial \bar{x}} + \frac{\partial \bar{u}}{\partial \bar{t}} = 0 \qquad (42)$$

State
$$\frac{\bar{p}}{\bar{\rho}^{\gamma}} = \text{const.} \qquad (43)$$

These can be put in more convenient form by introducing a new variable $\bar{v}$ defined as follows:

$$\bar{v} = \int_{\bar{\rho}_1}^{\bar{\rho}} \frac{\bar{c}}{\bar{\rho}}\,d\bar{\rho}, \qquad \frac{d\bar{v}}{d\bar{\rho}} = \frac{\bar{c}}{\bar{\rho}}, \qquad \frac{\partial}{\partial \bar{\rho}} = \frac{\bar{c}}{\bar{\rho}}\,\frac{\partial}{\partial \bar{v}}. \qquad (44)$$

For polytropic relation $\bar{p}/\bar{\rho}^{\gamma} = \text{const}$ we choose $\bar{\rho}_1 = 0$ and find

$$\bar{v} = \frac{2\bar{c}}{\gamma - 1}. \qquad (45)$$

When Equation (44) is substituted, Equations (41) and (42) read

$$\bar{c}\,\frac{\partial \bar{u}}{\partial \bar{x}} + \bar{u}\,\frac{\partial \bar{v}}{\partial \bar{x}} + \frac{\partial \bar{v}}{\partial \bar{t}} = 0 \qquad (41a)$$

$$\bar{u}\,\frac{\partial \bar{u}}{\partial \bar{x}} + \bar{c}\,\frac{\partial \bar{v}}{\partial \bar{x}} + \frac{\partial \bar{u}}{\partial \bar{t}} = 0. \qquad (42a)$$

These equations have characteristic directions

$$\frac{d\bar{x}}{d\bar{t}} = \bar{u} \pm \bar{c}. \tag{46}$$

Interchanging dependent and independent variables the x,t plane is mapped into the u,v or speedgraph plane (ref.2, p.160-171), and the equations of motion become

$$\bar{c}\,\frac{\partial\bar{t}}{\partial\bar{v}} - \bar{u}\,\frac{\partial\bar{t}}{\partial\bar{u}} + \frac{\partial\bar{x}}{\partial\bar{u}} = 0 \tag{47}$$

$$\bar{u}\,\frac{\partial\bar{t}}{\partial\bar{v}} - \bar{c}\,\frac{\partial\bar{t}}{\partial\bar{u}} - \frac{\partial\bar{x}}{\partial\bar{v}} = 0 \tag{48}$$

with characteristic directions

$$\frac{d\bar{v}}{d\bar{u}} = \pm 1. \tag{49}$$

Using $\bar{c}d\bar{\rho} = \bar{\rho}d\bar{v}$ Equations (47) and (48) may be written as

$$\frac{\partial}{\partial\bar{u}}(\bar{x}-\bar{u}\bar{t}) + \frac{\bar{c}}{\bar{\rho}}\,\frac{\partial}{\partial\bar{v}}\,(\bar{\rho}\bar{t}) = 0 \tag{50}$$

$$\frac{\partial}{\partial\bar{v}}\,(\bar{x}-\bar{u}\bar{t}) + \frac{\bar{c}}{\bar{\rho}}\,\frac{\partial}{\partial\bar{u}}\,(\bar{\rho}\bar{t}) = 0. \tag{51}$$

Equation (51) can be satisfied by setting

$$\bar{x} - \bar{u}\bar{t} = \frac{\partial V}{\partial \bar{u}}, \qquad \bar{t} = -\frac{1}{c}\frac{\partial V}{\partial \bar{v}} . \tag{52}$$

Then Equation (50) supplies the condition

$$\frac{\partial^2 V}{\partial \bar{v}^2} - \frac{\partial^2 V}{\partial \bar{u}^2} = \left(\frac{3-\gamma}{\gamma-1}\right)\frac{1}{\bar{v}}\frac{\partial V}{\partial \bar{v}} . \tag{53}$$

Restricting $3-\gamma/\gamma-1$ to integer values, m, Equation (53) can be written as

$$\frac{\partial^2 V}{\partial \bar{v}^2} - \frac{\partial^2 V}{\partial \bar{u}^2} = -\frac{2m}{\bar{v}}\frac{\partial V}{\partial \bar{v}} . \tag{53a}$$

The rest of this section will be devoted to the solution of Equation (53a) in Region III, with appropriate boundary conditions. The general solution of (53a) (ref.2, p.165) is

$$V_m = \bar{v}^{1-2m}\left[V_0 + \beta_1 \bar{v}V_0' + \beta_2 \bar{v}^2 V_0'' + \ldots + \beta_{m-1}\bar{v}^{(m-1)}V_0^{(m-1)}\right] \tag{54}$$

where

$$\beta_0 = 1, \qquad \beta_1 = 1$$

$$\beta_\nu = (-1)^\nu \frac{2^{\nu-1}}{\nu!} \frac{(m-2)(m-3)\ldots(m-\nu)}{(2m-3)(2m-4)\ldots(2m-\nu-1)}$$

$$V_0(\overline{u},\overline{v}) = f(\overline{v}+\overline{u}) + g(\overline{v}-\overline{u})$$

$$V_0'(\overline{u},\overline{v}) = f' + g'$$

f and g are arbitrary functions and the prime denotes differentiation with respect to the argument.

The particular cases $\gamma = 1.4$ and $\gamma = 3$ will now be considered.

(1)  $\underline{\gamma = 1.4}$

Inserting $\gamma = 1.4$ Equation (53a) becomes

$$\frac{\partial^2 V}{\partial \overline{v}^2} - \frac{\partial^2 V}{\partial \overline{u}^2} = -\frac{4}{\overline{v}} \frac{\partial V}{\partial \overline{v}} \tag{55}$$

while

$$\overline{v} = \frac{2\overline{c}}{\gamma-1} = 5\overline{c}.$$

It will be convenient to define two new variables

$$\xi = \overline{v} + \overline{u} \qquad \left( \text{Note: } \frac{\xi}{2} = \overline{r} \quad \text{where } \overline{r} \text{ and } \overline{s} \text{ are the Riemann invariants.} \right. $$

$$\left. \tag{56} \right.$$

$$\eta = \overline{v} - \overline{u} \qquad \frac{\eta}{2} = \overline{s}$$

It follows immediately that

$$\bar{v} = \frac{1}{2}(\xi+\eta)$$

$$\bar{u} = \frac{1}{2}(\xi-\eta). \tag{57}$$

From the general solution, Equation (54), we obtain

$$V = \frac{f(\xi)-\bar{v}f'(\xi)}{\bar{v}^3} + \frac{g(\eta)-\bar{v}g'(\eta)}{\bar{v}^3} \tag{58}.$$

and from Equation (52),

$$\bar{x} - \bar{u}\bar{t} = \frac{\partial V}{\partial \bar{u}} = \frac{f'(\xi)-\bar{v}f''(\xi)}{\bar{v}^3} - \frac{g'(\eta)-\bar{v}g''(\eta)}{\bar{v}^3} \tag{59}$$

$$\frac{\bar{v}\bar{t}}{s} = -\frac{\partial V}{\partial \bar{v}} = \frac{3f(\xi)-3\bar{v}f'(\xi)+\bar{v}^2f''(\xi)}{\bar{v}^4} + \frac{3g(\eta)-3\bar{v}g'(\eta)+\bar{v}^2g''(\eta)}{\bar{v}^4}$$

$$\tag{60}$$

For the wall boundary conditions we have $\bar{u} = 0$, $\bar{x} = 0$. (Here the origin has been translated so that $\bar{x} - 1 = \bar{x}$ where $\bar{x}$ is the length variable in Figure 2. Time $\bar{t}$ will be translated in the same way. These transformations simplify the algebra involved in obtaining a solution.)

From Equation (57) we obtain $\xi = \eta$ at the wall and inserting in (59)

$$\bar{x} - \bar{u}\bar{t} = 0 = \frac{\partial V}{\partial \bar{u}} = \frac{f'(\eta)-\bar{v}f''(\eta)}{\bar{v}^3} - \frac{g'(\eta)-\bar{v}g''(\eta)}{\bar{v}^3}$$

or

$$f'(\eta) - \bar{v}f''(\eta) = g'(\eta) - \bar{v}g''(\eta). \tag{61}$$

This has the general solution

$$f(\eta) = g(\eta) + c_1\eta^2 + c_2.$$

Since we are interested in a particular solution we shall set $c_1 = 0$, $c_2 = 0$ giving

$$f(\eta) = g(\eta). \tag{62}$$

As mentioned previously two different assumptions were made concerning the shock boundary; the first was $\bar{s} = \bar{s}_0$, a constant, on the shock, the second was $\bar{s} = \bar{s}_1 + \alpha\bar{r}$ on the shock. Both will now be considered.

a.  $\underline{\bar{s} = \bar{s}_0}$

If $\bar{s} = \bar{s}_0$ then by Equation (56) $\eta = \text{const} = \eta_1$ and by Equation (57) $\bar{v} = 1/2(\xi + \eta_1)$ on the shock. From the data of Whithams solution it is possible to represent the time on the shock curve by

$$\bar{t} = \sum_0^4 b_n \, \xi^n - 1 . \tag{63}$$

Substituting in Equation (60) we have on the shock

$$\frac{\xi+\eta_1}{10}\left(\sum_0^4 b_n\xi^n -1\right) = \frac{3f(\xi)-3/2(\xi+\eta_1)f'(\xi)+1/4(\xi+\eta_1)^2 f''(\xi)}{1/16(\xi+\eta_1)^4}$$

$$+ \frac{3g_1-3/2(\xi+\eta_1)g_1'+1/4(\xi+\eta_1)^2 g_1''}{1/16(\xi+\eta_1)^4} \qquad (64)$$

where $g(\eta_1) = g_1$, etc.

This has a solution (ref.2, p.175)

$$f(\xi) = \frac{(\xi+\eta_1)^4}{4} A\left[\frac{1}{2}(\xi+\eta_1)\right] - g_1 + (\xi+\eta_1)g_1' - \frac{1}{2}(\xi+\eta_1)^2 g_1''$$

$$(65)$$

with arbitrary constants $g_1$, $g_1'$, $g_1''$ and where

$$A = \frac{1}{5}\int_{\overline{v}_1}^{\overline{v}} (1 - \frac{z}{v})\overline{t}(z)dz. \qquad (66)$$

We can also obtain

$$f'(\xi) = (\xi+\eta_1)^3 A + \frac{(\xi+\eta_1)^4}{8} A' + g_1' - (\xi+\eta_1)g_1'' \qquad (67)$$

$$f''(\xi) = 3(\xi+\eta_1)^2 A + (\xi+\eta_1)^3 A' + \frac{(\xi+\eta_1)^4}{16} A'' - g_1'' \qquad (68)$$

24

Evaluating these equations at $\xi = \xi_1 = \eta_1$ we find they are homogeneous in the constants and therefore all constants can be set equal zero and

$$f(\xi) = \frac{(\xi+\eta_1)^4}{4} \, A\left[\frac{1}{2}(\xi+\eta_1)\right]. \tag{69}$$

Integrating Equation (66), using Equation (63) for $\bar{t}$ one obtains

$$A = \frac{1}{10(\xi+\eta_1)} \left[ \sum_0^4 \frac{b_n \xi^{n+2}}{(n+1)(n+2)} - \frac{1}{2}\xi^2 + \left(\xi_1 - \sum_0^4 \frac{b_n \xi_1^{n+1}}{n+1}\right)\xi \right.$$
$$\left. + \left(\sum_0^4 \frac{b_n \xi_1^{n+2}}{n+2} - \frac{1}{2}\xi_1^2\right) \right] \tag{70}$$

Thus with Equations (59), (60), (69), and (70) we have the complete solution to the problem.

b.    $\bar{s} = \bar{s}_1 + \alpha\bar{r}$

If $\bar{s} = \bar{s}_1 + \alpha\bar{r}$, then by (56) and (57) the following apply on the shock boundary:

$$\eta = a + b\xi \qquad (\text{where } a = 2\bar{s}_1, \ b = \alpha) \tag{71}$$

$$\bar{v} = 1/2[a + (1+b)\xi]. \tag{72}$$

25

$\overline{s}_1$ and $\alpha$ are obtained from the Whitham solution. The time t on the shock can be represented by a quadratic with less than 1 percent error.

$$\overline{t} = \sum_{0}^{2} d_n \, \xi^n - 1. \tag{73}$$

Equation (60) now becomes [using (62) and (71)]

$$\frac{1}{10}[a+(1+b)\xi]\left(\sum_{0}^{2} d_n \xi^{n-1}\right) =$$

$$\left\{3[f(\xi)+f(a+b\xi)] - \frac{3}{2}[a+(1+b)\xi][f'(\xi)+f'(a+b\xi)]\right.$$

$$\left. + \frac{1}{4}[a+(1+b)\xi]^2[f''(\xi)+f''(a+b\xi)]\right\} \Big/ \frac{1}{16}[a+(1+b)\xi]^4 \tag{74}$$

This is a mixed differential-difference equation and it can be seen by inspection that a solution is

$$f(\xi) = \sum_{0}^{7} P_n \, \xi^n \tag{75}$$

and by (62)

$$g(\eta) = \sum_{0}^{7} P_n \eta^n. \tag{76}$$

On the shock

$$g(\eta) = f(\eta) = f(a+b\xi) = \sum_{0}^{7} P_n(a+b\xi)^n. \tag{77}$$

Substituting Equations (75) and (77) into (74) and equating coefficients of like powers of $\xi$ to zero one obtains eight equations for the eight unknown coefficients, $P_n$. For this particular problem b is a small number hence terms in $b^2$ on higher powers were ignored (the problem was also done retaining terms in $b^2$ with a negligible change in results). With the $P_n$'s determined the entire solution is in hand. Expressions for the $P_n$'s are given in Appendix I.

(2)  $\underline{\gamma = 3}$

Inserting $\gamma = 3$, Equation (53) becomes the wave equation:

$$\frac{\partial^2 V}{\partial \bar{v}^2} - \frac{\partial^2 V}{\partial \bar{u}^2} = 0 \tag{78}$$

while $\bar{v} = \dfrac{2\bar{c}}{\gamma-1} = \bar{c}$. Using the definitions of Equations (56), the general solution to (78) can be written as

$$V = f(\xi) + g(\eta). \tag{79}$$

From Equation (52)

$$\overline{x} = \overline{ut} = f'(\xi) - g'(\eta) \tag{80}$$

$$\overline{ct} = -[f'(\xi)+g'(\eta)] \; . \tag{81}$$

The wall boundary condition again yields

$$f(\eta) = g(\eta). \tag{62}$$

As in the case of $\gamma = 1.4$ we shall consider both $\overline{s} = \overline{s}_0$ on the shock and $\overline{s} = \overline{s}_1 + \alpha \overline{r}$ on the shock. $\overline{s}_0$, $\overline{s}_1$ and $\alpha$ are determined from the $\gamma = 3$ Whitham shock solution.

a.   $\underline{\overline{s} = \overline{s}_0}$

Again $\eta = \eta_1$ a constant and $\overline{v} = 1/2(\xi+\eta_1)$ on the shock. Also on the shock

$$\overline{t} = \sum_0^4 d_n \xi^n - 1. \tag{82}$$

Substituting (82) into (81), with $\eta = \eta_1$

$$f'(\xi) = -\frac{1}{2}(\xi+\eta_1)\left(\sum_0^4 d_n\xi^n-1\right) - g'_1$$

and the desired particular solution is

$$f(\xi) = \frac{1}{2} \int_{\xi_1}^{\xi} (\xi + \eta_1) \left( 1 - \sum_0^4 d_n \xi^n \right) d\xi$$

or

$$f(\xi) = \frac{1}{2} \left\{ -\sum_0^4 d_n \frac{\xi^{n+2}}{n+2} - \xi_1 \sum_0^4 d_n \frac{\xi^{n+1}}{n+1} + \frac{1}{2}\xi^2 + \xi_1\xi \right.$$

$$\left. + \left[ \sum_0^4 d_n \frac{(2n+3)}{(n+2)(n+1)} \xi_1^{n+2} - \frac{3}{2}\xi_1^2 \right] \right\} . \qquad (83)$$

Thus Equations (62), (80), (81), and (83) afford the complete solution.

b.   $\overline{s} = \overline{s}_1 + \alpha\overline{r}$

As in the case of $\gamma = 1.4$ Equations (62), (71) and (72) apply, with a and b now determined by the $\gamma = 3$ shock solution.  For $\overline{t}$ we have

$$t = \sum_0^4 d_n \xi^n - 1. \qquad (84)$$

Equation (81) on the shock becomes

$$\frac{1}{2}[a + (1+b)\xi] \left( \sum_0^4 d_n \xi^n - 1 \right) = -f'(\xi) - f'(a+b\xi) \qquad (85)$$

A solution of the mixed differential difference equation is

$$f'(\xi) = \sum_0^5 P_n \xi^n \qquad (86)$$

and by (62)

$$g'(\eta) = \sum_0^5 P_n \eta^n, \tag{87}$$

however on the shock

$$g'(\eta) = f'(\eta) = f'(a+b\xi) = \sum_0^5 P_n(a+b\xi)^n \tag{88}$$

Introducing Equations (86) and (88) into (85) and equating coefficients of like powers of $\xi$ to zero one obtains six equations for the six $P_n$'s and hence has the complete solution. Expressions for the $P_n$'s are given in Appendix I.

Two other approximate solutions were obtained for $\gamma = 3$. They are as follows.

c. <u>Extend $C^+$ Characteristics from Region II into Region III</u>

For $\gamma = 3$ both the $C^+$ and $C^-$ characteristics are straight lines in an isentropic region. The simplest approximation to this problem is therefore to ignore the reflected shock and carry the straight $C^+$ characteristics of Region II into Region III. The equation of these characteristics is

$$\frac{\bar{x}}{\bar{t}} = \bar{u} + \bar{c} \tag{89}$$

At the wall $\bar{x} = 1$ (using the coordinates of Figure 2). Also at the wall $\bar{u} = 0$, hence

$$\bar{c}_{wall} = \frac{1}{\bar{t}_{wall}} .$$ (90)

The adiabatic relation, 4, then enables one to calculate wall pressure versus time.

d. <u>Extend $C^+$ Characteristics from Whithan Shock Curve</u>

Another relatively simple method of computing the flow in Region III is to utilize the entire Whitham shock solution. This solution yields u and c as functions of position along the shock. Assuming isentropic flow behind the shock means the $C^+$ characteristics behind the shock are straight and can be represented by

$$\frac{\bar{x} - \bar{x}_0}{\bar{t} - \bar{t}_0} = \bar{u} + \bar{c}$$ (91)

also

$$\bar{u} + \bar{c} = \bar{u}_0 + \bar{c}_0 = \bar{r}_0$$ (92)

where the subscript 0 refers to the shock. Combining (91) and (92) we obtain

$$\bar{x} - \bar{x}_0 = 2(\bar{t} - \bar{t}_0)\bar{r}_0 \tag{93}$$

but on the shock $\bar{r}_0 = \bar{r}_0(\bar{t}_0)$, $\bar{x}_0 = \bar{x}_0(\bar{t}_0)$; both known functions. On the wall $\bar{x} = 1$ so that

$$\bar{t}_{wall} = \bar{t}_0 + \frac{1 - \bar{x}_0(\bar{t}_0)}{2\bar{r}_0(\bar{t}_0)} . \tag{94}$$

Also on the wall $\bar{u} = 0$ and therefore

$$\bar{c}_{wall} = 2\bar{r}_0(\bar{t}_0) . \tag{95}$$

Equations (94) and (95) together with the adiabatic relation 4 then give the wall pressure versus time.

## 3. RESULTS

Figure 3 shows the shock paths given by the Whitham solution for adiabatic exponents of 1.4, 2.2, and 3.0. Tables 1, 2, and 3 contain the shock data necessary to obtain a solution in Region III. It is of interest to note that as the shock strengthens at the tail of the rarefaction a discontinuity develops in the flow behind the shock for $\gamma > 2$. This discontinuity appears to be the beginning of another shock directed back into the flow and toward the wall. That this flow pattern is not just a result of the approximate method of calculation is demonstrated in Appendix II.

32
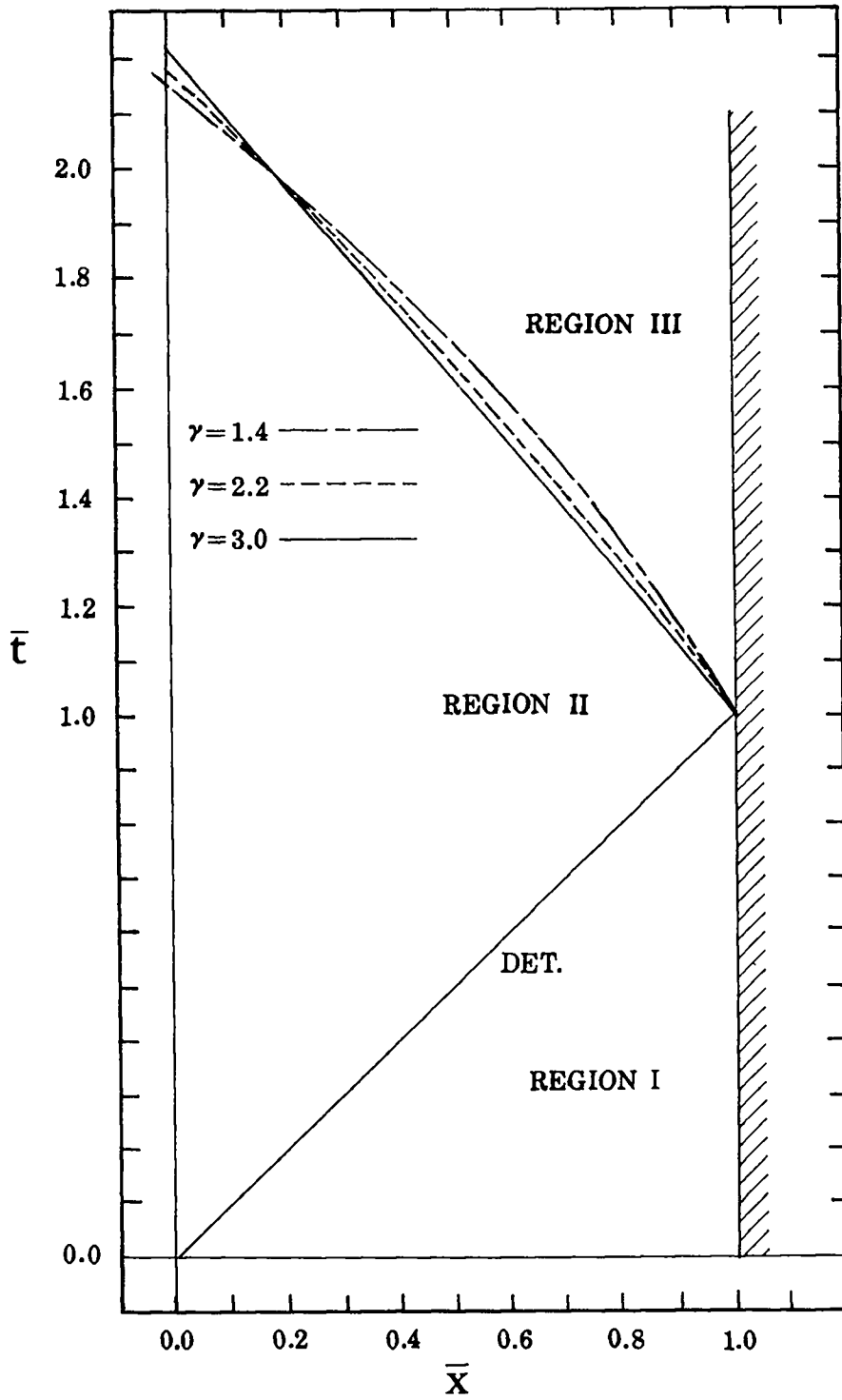
Figure 3. Shock Paths Computed by Whitham Method for $\gamma$=1.4, 2.2, 3.0.

Table 1. Reflected Shock Data $\gamma = 1.4$

| $\bar{t}$ | $\bar{x}$ | $\bar{U}$ | $\bar{u}$ | $\bar{c}$ | $\bar{r}$ | $\bar{s}$ |
|-----------|-----------|-----------|-----------|-----------|-----------|-----------|
| 1.000 | 1.000 | -0.468 | 0.000 | 0.673 | 1.683 | 1.683 |
| 1.193 | 0.893 | -0.641 | -0.211 | 0.632 | 1.475 | 1.687 |
| 1.327 | 0.800 | -0.741 | -0.334 | 0.609 | 1.356 | 1.690 |
| 1.461 | 0.694 | -0.830 | -0.442 | 0.589 | 1.251 | 1.693 |
| 1.580 | 0.591 | -0.900 | -0.527 | 0.573 | 1.168 | 1.696 |
| 1.685 | 0.494 | -0.956 | -0.595 | 0.560 | 1.102 | 1.698 |
| 1.789 | 0.391 | -1.009 | -0.659 | 0.548 | 1.042 | 1.700 |
| 1.879 | 0.299 | -1.050 | -0.709 | 0.539 | 0.993 | 1.702 |
| 1.984 | 0.186 | -1.096 | -0.764 | 0.529 | 0.940 | 1.704 |
| 2.073 | 0.086 | -1.333 | -0.809 | 0.521 | 0.898 | 1.706 |
| 2.163 | -0.017 | -1.168 | -0.851 | 0.513 | 0.858 | 1.708 |

Least Squares Polynomial Fit to Some of the Above Data

4th Degree $\quad \bar{t} = 5.942 - 7.393\,\bar{r} + 4.673\,\bar{r}^2 - 1.581\,\bar{r}^3 + 0.224\,\bar{r}^4$

2nd Degree $\quad \bar{t} + 4.599 - 3.596\,\bar{r} + 0.868\,\bar{r}^2$

$\qquad\qquad \bar{s} = 1.734 - 0.032\,\bar{r}$

Table 2.  Reflected Shock Data  $\gamma = 2.2$

| $\bar{t}$ | $\bar{x}$ | $\bar{U}$ | $\bar{u}$ | $\bar{c}$ | $\bar{r}$ | $\bar{s}$ |
|-------|--------|--------|--------|-------|-------|-------|
| 1.000 | 1.000 | -0.669 | 0.000 | 0.884 | 0.737 | 0.737 |
| 1.144 | 0.899 | -0.729 | -0.134 | 0.807 | 0.605 | 0.740 |
| 1.289 | 0.798 | -0.775 | -0.237 | 0.749 | 0.506 | 0.742 |
| 1.405 | 0.698 | -0.813 | -0.317 | 0.704 | 0.428 | 0.745 |
| 1.525 | 0.598 | -0.844 | -0.383 | 0.668 | 0.365 | 0.748 |
| 1.642 | 0.498 | -0.872 | -0.440 | 0.637 | 0.311 | 0.751 |
| 1.753 | 0.400 | -0.896 | -0.488 | 0.612 | 0.266 | 0.754 |
| 1.864 | 0.299 | -0.919 | -0.531 | 0.590 | 0.226 | 0.757 |
| 1.972 | 0.199 | -0.939 | -0.569 | 0.571 | 0.191 | 0.761 |
| 2.077 | 0.099 | -0.958 | -0.604 | 0.555 | 0.160 | 0.764 |
| 2.181 | -0.002 | -0.976 | -0.635 | 0.540 | 0.132 | 0.768 |

### Table 3. Reflected Shock Data $\gamma = 3.0$

| $\bar{t}$ | $\bar{x}$ | $\bar{U}$ | $\bar{u}$ | $\bar{c}$ | $\bar{r}$ | $\bar{s}$ |
|-----------|-----------|-----------|-----------|-----------|-----------|-----------|
| 1.000 | 1.000 | -0.791 | 0.000 | 1.010 | 0.505 | 0.505 |
| 1.129 | 0.898 | -0.797 | -0.103 | 0.911 | 0.404 | 0.507 |
| 1.252 | 0.799 | -0.803 | -0.181 | 0.836 | 0.327 | 0.508 |
| 1.378 | 0.698 | -0.810 | -0.248 | 0.773 | 0.263 | 0.511 |
| 1.501 | 0.598 | -0.817 | -0.302 | 0.723 | 0.211 | 0.513 |
| 1.621 | 0.499 | -0.824 | -0.348 | 0.683 | 0.168 | 0.515 |
| 1.741 | 0.400 | -0.831 | -0.387 | 0.649 | 0.131 | 0.518 |
| 1.861 | 0.300 | -0.839 | -0.422 | 0.620 | 0.099 | 0.521 |
| 1.981 | 0.199 | -0.847 | -0.454 | 0.595 | 0.071 | 0.524 |
| 2.098 | 0.099 | -0.855 | -0.481 | 0.575 | 0.047 | 0.528 |
| 2.215 | -0.001 | -0.864 | -0.506 | 0.557 | 0.026 | 0.532 |

Least Squares Polynomial Fit to Some of the Above Data ($1. \leq t \leq 1.741$)

$$\bar{t} = 2.357 - 6.185\,\bar{r} + 13.477\,\bar{r}^2 - 18.585\,\bar{r}^3 + 11.122\,\bar{r}^4$$

$$\bar{s} = 0.525 - 0.046\,\bar{r}$$

The solutions in Region III are characterized by plots of recomputed "shock" paths (those determined by the isentropic solution in Region III) and plots of wall pressure versus time, Figures 4 through 7. The numerical data for these solutions are given in Tables 4 and 5.

Figure 4, $\gamma = 1.4$, shows that the more refined approximation $(\bar{s} = \bar{s}_1 + \alpha\bar{r}$ as opposed to $\bar{s} = \bar{s}_0)$ resulted in a shock curve further removed from the Whitham curve than the characteristic approximation, although the difference is extremely small. Neither are in very satisfactory agreement with the Whitham solution.

Figure 5 compares the wall pressure calculated by letting $\bar{s} = \bar{s}_0$ and $\bar{s} = \bar{s}_1 + \alpha\bar{r}$. Here again the difference is negligible.

For $\gamma = 3$ the different methods produce significantly different shock curves. Figure 6 compares the Whitham shock, the $\bar{s} = \bar{s}_1 + \alpha\bar{r}$ curve, and the $\bar{s} = \bar{s}_0$ curve. The $\bar{s} = \bar{s}_1 + \alpha\bar{r}$ curve is a considerable improvement over the characteristic approximation although still leaving much to be desired.

Figure 7 shows that, as for $\gamma = 1.4$, there is little to difference between the $\bar{s} = \bar{s}_0$ and $\bar{s} = \bar{s}_1 + \alpha\bar{r}$ pressure distributions. Both, however, yield pressures which decay noticeably slower than those obtained either by extending the $C^+$ characteristics from Region II to Region III or by continuing the $C^+$ characteristics from the shock, using slopes obtained from the shock solution.

It would appear that the simpler approximations for $\gamma = 3$ are somewhat conservative and that on the whole the wall pressure profile
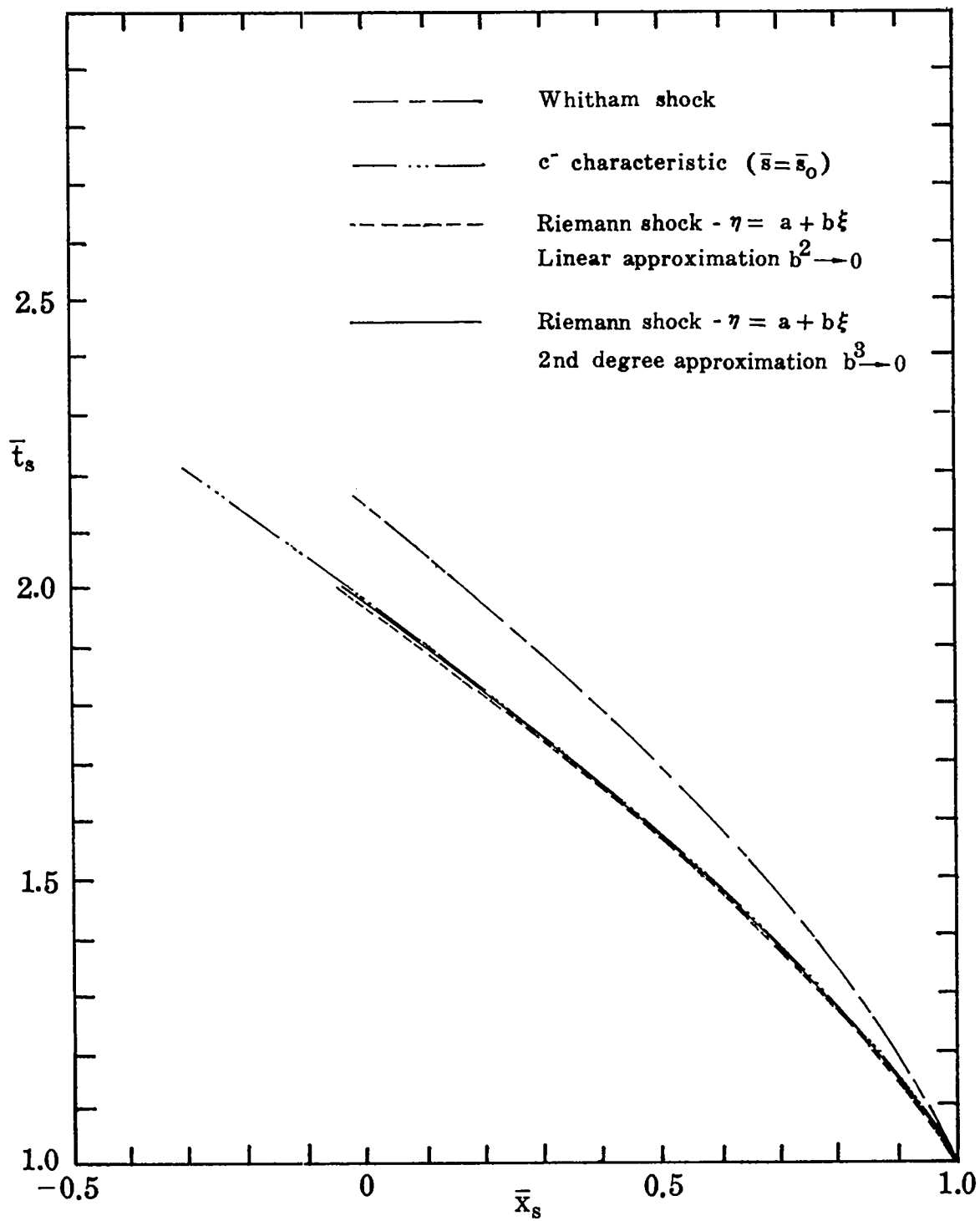
Figure 4. Shock or Characteristic Path  $\gamma = 1.4$

Riemann shock - $\eta = a + b\xi$
2nd degree approximation $b^3 \to 0$

Riemann shock - $\eta = a + b\xi$
Linear approximation $b^2 \to 0$

Riemann characteristic

⊙    From Circe $\gamma = 1.4$; scaled to read $\bar{p}_w = .05683$ at $\bar{t}_w = 1$

$\bar{p}_w \times 10^{-2}$

$\bar{t}_w$
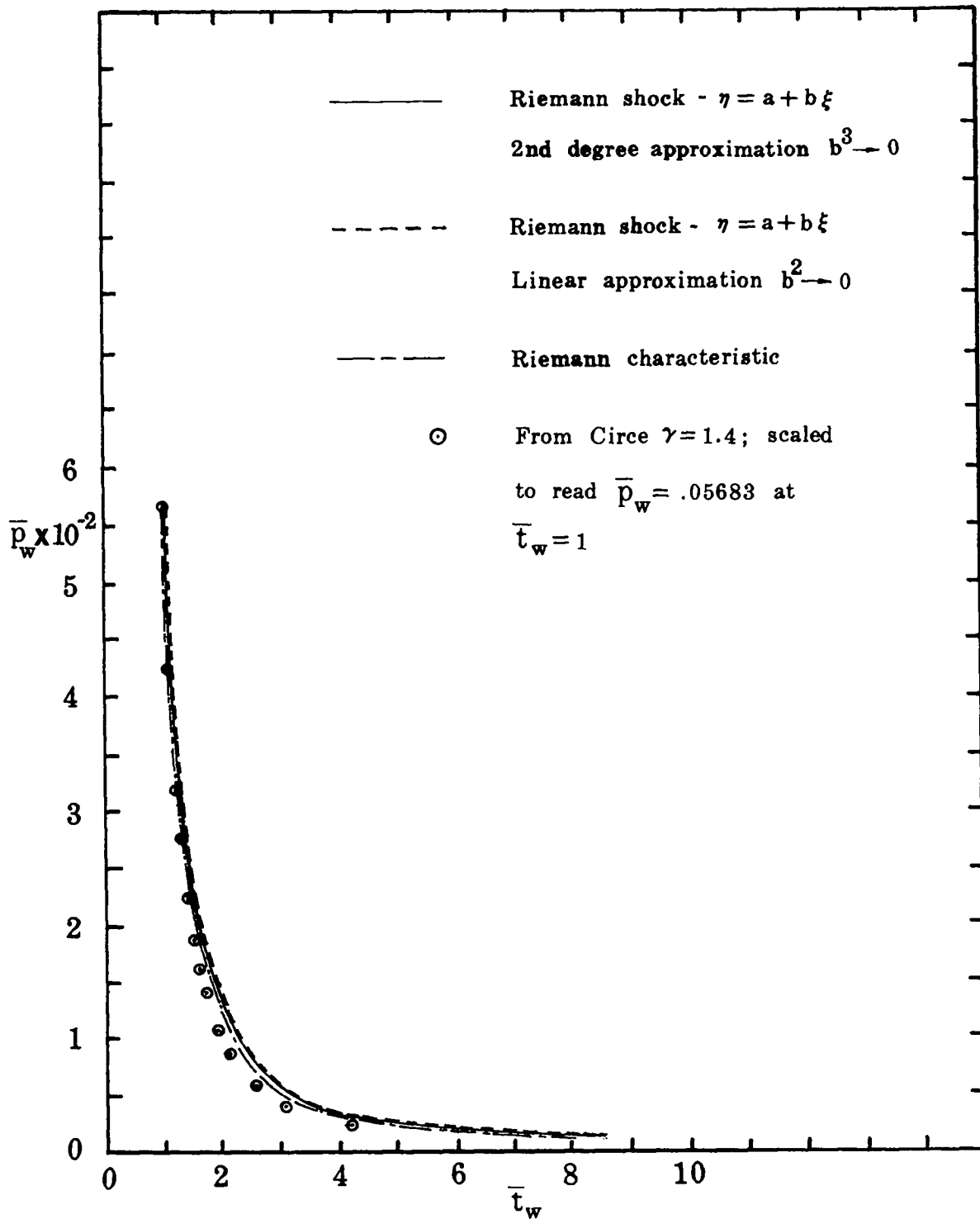
Figure 5. Wall Pressure vs. Time   $\gamma = 1.4$

Table 4.  Data From Solution in Region III    $\gamma = 1.4$

$$\bar{s} = \bar{s}_0 = 1.683$$

| Shock Curve | | Wall Pressure | |
|---|---|---|---|
| $\bar{t}_s$ | $\bar{x}_s$ | $\bar{t}_w$ | $\bar{P}_w$ |
| 1.000 | 1.000 | 1.000 | $5.683 \times 10^{-2}$ |
| 1.100 | 0.928 | 1.154 | $4.000 \times 10^{-2}$ |
| 1.200 | 0.847 | 1.354 | $2.759 \times 10^{-2}$ |
| 1.300 | 0.759 | 1.617 | $1.865 \times 10^{-2}$ |
| 1.400 | 0.663 | 1.971 | $1.232 \times 10^{-2}$ |
| 1.500 | 0.561 | 2.459 | $0.793 \times 10^{-2}$ |
| 1.600 | 0.453 | 3.151 | $0.496 \times 10^{-2}$ |
| 1.700 | 0.340 | 4.162 | $0.299 \times 10^{-2}$ |
| 1.800 | 0.222 | 5.694 | $0.174 \times 10^{-2}$ |
| 1.900 | 0.099 | 8.104 | $0.096 \times 10^{-2}$ |
| 2.000 | -0.028 | | |

Note:  $\bar{P}_w = \dfrac{p_w}{\rho_0 D^2}$

## Table 4. Continued

$$\bar{s} = \bar{s}_1 + \alpha \bar{r}$$

$$\bar{s}_1 = 1.734, \ \alpha = -0.032$$

$$P_0 = 4.6030, \ P_1 = 0, \ P_2 = -1.1122, \ P_3 = 0, \ P_4 = 0.0896,$$

$$P_5 = -0.0148, \ P_6 = -0.0027, \ P_7 = 0.0004$$

| Shock Curve | | Wall Pressure | |
|---|---|---|---|
| $\bar{t}_s$ | $\bar{x}_s$ | $\bar{t}_w$ | $\bar{p}_w$ |
| 1.007 | 1.001 | 1.033 | $5.683 \times 10^{-2}$ |
| 1.068 | 0.958 | 1.169 | $3.997 \times 10^{-2}$ |
| 1.142 | 0.901 | 1.358 | $2.759 \times 10^{-2}$ |
| 1.227 | 0.829 | 1.621 | $1.865 \times 10^{-2}$ |
| 1.324 | 0.739 | 1.986 | $1.232 \times 10^{-2}$ |
| 1.433 | 0.631 | 2.498 | $0.793 \times 10^{-2}$ |
| 1.553 | 0.502 | 3.227 | $0.496 \times 10^{-2}$ |
| 1.686 | 0.351 | 4.293 | $0.299 \times 10^{-2}$ |
| 1.830 | 0.175 | 5.898 | $0.174 \times 10^{-2}$ |
| 1.986 | -0.026 | 8.407 | $0.096 \times 10^{-2}$ |
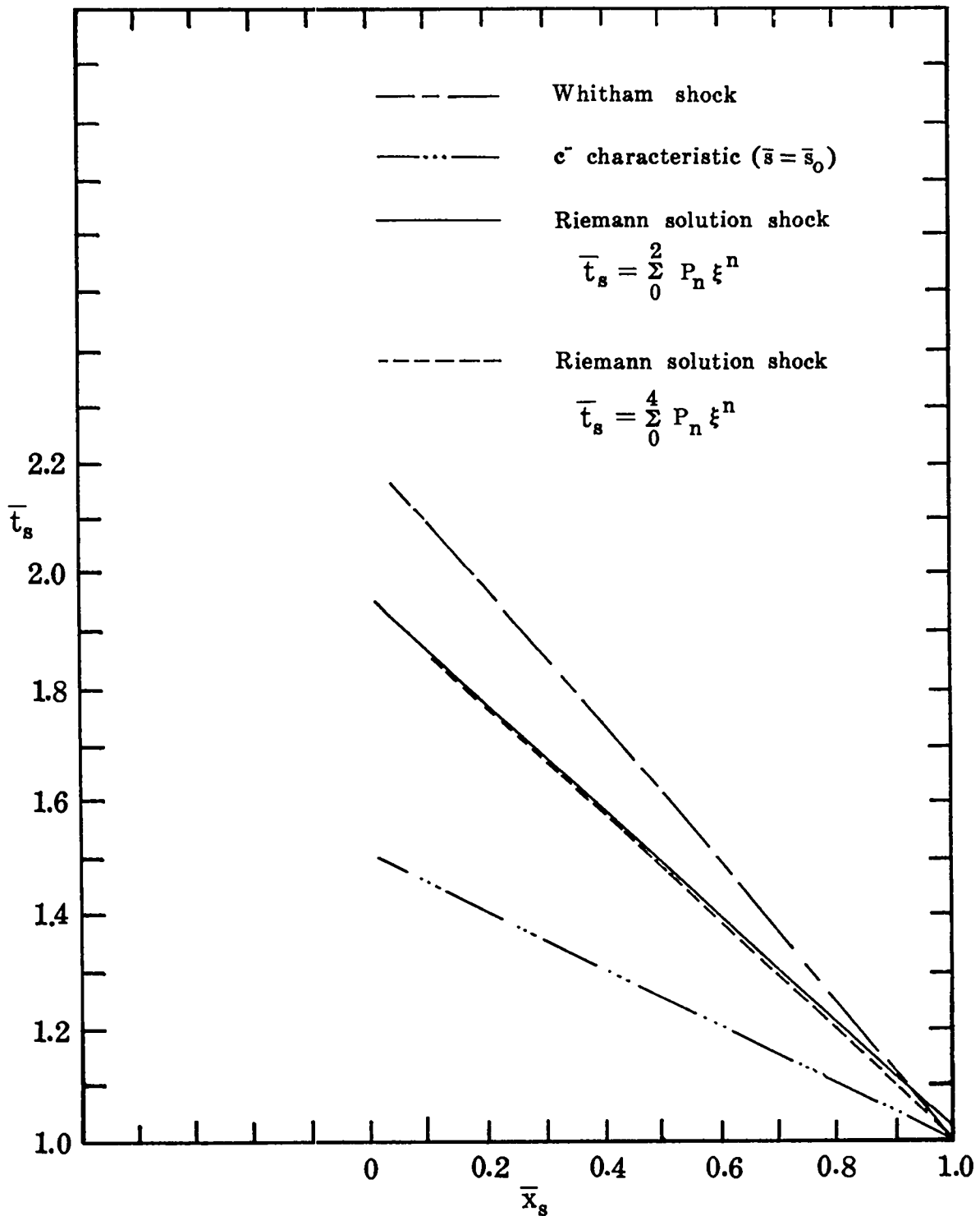
Figure 6. Shock or Characteristic Path $\gamma=3.0$

The legend of the figure reads:

- — - — Whitham shock
- —···— $c^-$ characteristic ($\bar{s} = \bar{s}_0$)
- —— Riemann solution shock $\bar{t}_s = \overset{2}{\underset{0}{\Sigma}} P_n \xi^n$
- - - - - Riemann solution shock $\bar{t}_s = \overset{4}{\underset{0}{\Sigma}} P_n \xi^n$

The vertical axis is labeled $\bar{t}_s$ with values 1.0, 1.2, 1.4, 1.6, 1.8, 2.0, 2.2.

The horizontal axis is labeled $\bar{x}_s$ with values 0, 0.2, 0.4, 0.6, 0.8, 1.0.

2.5

Continuation of original characteristics.

Whitham shock solution characteristics extended from shock.

Whitham shock data put on $c^-$ characteristic. Riemann solution.

Whitham shock data and Riemann solution on shock

$$\overline{t}_s = \sum_0^4 P_n \xi^n$$

⊙   From Circe $\gamma = 3$; scaled to read $\overline{p}_w = .2235$ at $\overline{t}_w = 1$

$\overline{p}_w \times 10^{-1}$

2.0

1.5

1.0

0.5

0.0

1          2          3          4

$\overline{t}_w$
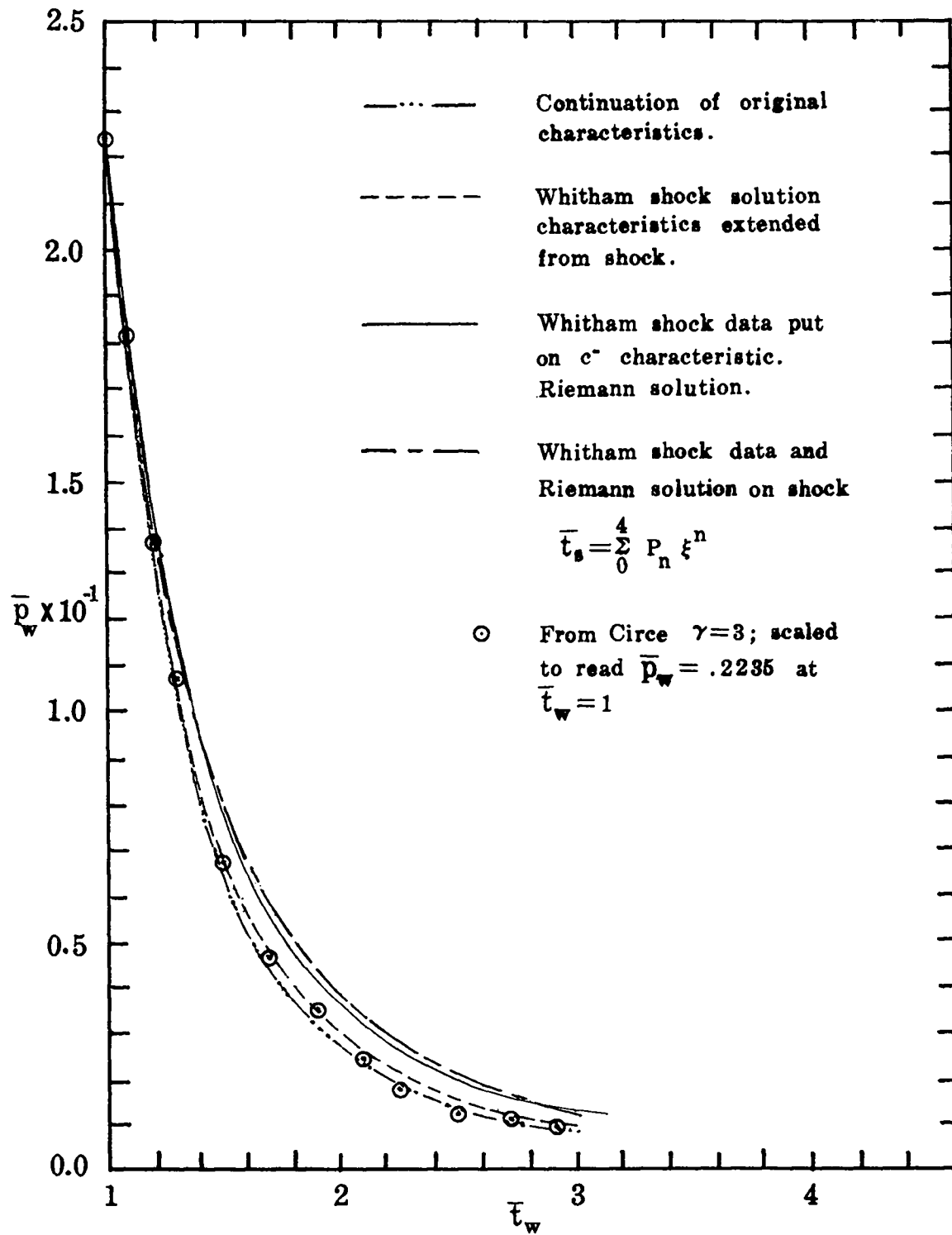
Figure 7.  Wall Pressure vs. Time   $\gamma = 3.0$

Table 5.   Data From Solution in Region III   $\gamma = 3.0$

$$\bar{s} = \bar{s}_0 = 0.505$$

| Shock Curve | | Wall Pressure | |
|---|---|---|---|
| $\bar{t}_s$ | $\bar{x}_s$ | $\bar{t}_w$ | $\bar{p}_w$ |
| 1.000 | 1.000 | 1.001 | $2.235 \times 10^{-1}$ |
| 1.100 | 0.802 | 1.110 | $1.689 \times 10^{-1}$ |
| 1.200 | 0.604 | 1.250 | $1.240 \times 10^{-1}$ |
| 1.300 | 0.406 | 1.427 | $0.879 \times 10^{-1}$ |
| 1.400 | 0.208 | 1.655 | $0.596 \times 10^{-1}$ |
| 1.500 | 0.010 | 1.959 | $0.381 \times 10^{-1}$ |
| 1.600 | -0.188 | 2.387 | $0.225 \times 10^{-1}$ |
| 1.700 | -0.386 | 3.031 | $0.119 \times 10^{-1}$ |
| 1.800 | -0.584 | 4.100 | $0.053 \times 10^{-1}$ |
| 1.900 | -0.782 | 6.175 | $0.017 \times 10^{-1}$ |
| 2.00 | -0.980 | 11.727 | $0.003 \times 10^{-1}$ |

## Table 5. Continued

$$\bar{s} = \bar{s}_1 + \alpha\bar{r}$$

$$\bar{s}_1 = 0.525, \ \alpha = -0.046$$

$$P_0 = -0.7352, \ P_1 = 0.9996, \ P_2 = -0.2918,$$

$$P_3 = -0.3884, \ P_4 = 0.7435$$

| Shock Curve | | Wall Pressure | |
|---|---|---|---|
| $\bar{t}_s$ | $\bar{x}_s$ | $\bar{t}_w$ | $\bar{p}_w$ |
| 1.000 | 1.000 | 0.996 | $2.235 \times 10^{-1}$ |
| 1.053 | 0.947 | 1.111 | $1.689 \times 10^{-1}$ |
| 1.113 | 0.886 | 1.256 | $1.240 \times 10^{-1}$ |
| 1.181 | 0.817 | 1.441 | $0.879 \times 10^{-1}$ |
| 1.256 | 0.739 | 1.680 | $0.596 \times 10^{-1}$ |
| 1.342 | 0.650 | 2.001 | $0.381 \times 10^{-1}$ |
| 1.440 | 0.547 | 2.453 | $0.225 \times 10^{-1}$ |
| 1.555 | 0.427 | 3.136 | $0.119 \times 10^{-1}$ |
| 1.692 | 0.283 | 4.273 | $0.053 \times 10^{-1}$ |
| 1.856 | 0.110 | 6.487 | $0.017 \times 10^{-1}$ |

## Table 5. Continued

### Continuation of Region II Characteristics
### No Reflected Shock to Consider

#### Wall Pressure

| $\bar{t}_w$ | $\bar{p}_w$ |
|---|---|
| 1.000 | $2.169 \times 10^{-1}$ |
| 1.200 | $1.255 \times 10^{-1}$ |
| 1.400 | $0.790 \times 10^{-1}$ |
| 1.600 | $0.529 \times 10^{-1}$ |
| 1.800 | $0.372 \times 10^{-1}$ |
| 2.000 | $0.271 \times 10^{-1}$ |
| 2.200 | $0.204 \times 10^{-1}$ |
| 2.400 | $0.157 \times 10^{-1}$ |
| 2.600 | $0.123 \times 10^{-1}$ |
| 2.800 | $0.099 \times 10^{-1}$ |
| 3.000 | $0.080 \times 10^{-1}$ |

Table 5. Continued

Utilizing $\bar{u}$ and $\bar{c}$ From Whitham Shock Solution Extend
Straight $C^+$ Characteristics From Shock Into Region III.
Shock Curve Given In Table 3.

Wall Pressure

| $\bar{t}_w$ | $\bar{p}_w$ |
|---|---|
| 1.000 | $2.232 \times 10^{-1}$ |
| 1.112 | $1.636 \times 10^{-1}$ |
| 1.236 | $1.200 \times 10^{-1}$ |
| 1.373 | $0.881 \times 10^{-1}$ |
| 1.526 | $0.646 \times 10^{-1}$ |
| 1.698 | $0.473 \times 10^{-1}$ |
| 1.891 | $0.346 \times 10^{-1}$ |
| 2.110 | $0.251 \times 10^{-1}$ |
| 2.360 | $0.182 \times 10^{-1}$ |
| 2.649 | $0.130 \times 10^{-1}$ |
| 2.984 | $0.093 \times 10^{-1}$ |

is rather insensitive to slight modifications in methods of calculation.

The large discrepancy in shock curves apparently results from the assumption of isentropic flow behind the shock, although the approximate character of the Whitham solution may make some contribution.

In the discussion to this point the Whitham shock curve has been considered an adequate approximation to the actual shock path. For $\gamma = 1.4$ and $\gamma = 3.0$ a comparison was made between the Whitham solution and the solution to the same problem using a numerical code (Circe). The numerical method uses a one-dimensional Lagrangian approach with a pseudo-viscosity term to give a smeared shock. Data for the Circe results are given in Tables 6 and 7 for $\gamma = 1.4$ and $\gamma = 3.0$ respectively. Figures 8 and 9 compare the Whitham and Circe shock curves. It is apparent that the Whitham shock accelerates much too rapidly. A third calculation was made for $\gamma = 3.0$, namely a graphical-characteristic integration for the shock and flow field between the shock and wall (see Appendix III for details); data for this are contained in Table 8. Figure 10 illustrates the three shock curves for $\gamma = 3.0$. The graphic solution appears to confirm the Circe result; also the Whitham solution and the graphical solution have opposite curvature which implies the continued divergence of the two curves.

Scaled Circe pressure profiles are plotted in Figures 5 and 7. These curves appear to confirm a previous conclusion, namely that the pressure profiles are relatively insensitive to variations in the shock path.

48

Table 6. Reflected Shock Data   Circe OT682  $\gamma = 1.4$  Sharp Detonation

| t | x | $u_s$ | $c_s$ | $dx/dt = u_s + c_s$ (behind shock) | $p_{wall}$ (megabars) |
|---|---|---|---|---|---|
| 1.070 | 0.967 | -0.0337 | 0.654 | 0.620 | 0.854 |
| 1.173 | 0.914 | -0.116 | 0.625 | 0.509 | 0.659 |
| 1.275 | 0.847 | -0.208 | 0.610 | 0.402 | 0.525 |
| 1.377 | 0.781 | -0.266 | 0.585 | 0.319 | 0.427 |
| 1.582 | 0.623 | -0.388 | 0.555 | 0.167 | 0.300 |
| 1.787 | 0.452 | -0.520 | 0.532 | 0.012 | 0.223 |
| 2.094 | 0.160 | -0.652 | 0.500 | -0.152 | 0.155 |
| 2.401 | -0.178 | -0.743 | 0.473 | -0.270 | 0.114 |
| 2.709 | -0.513 | -0.814 | 0.446 | -0.368 | 0.0885 |
| 3.016 | -0.868 | -0.913 | 0.434 | -0.479 | 0.0709 |
| 3.323 | -1.265 | -0.955 | 0.411 | -0.544 | 0.0583 |
| 3.630 | -1.661 | -1.015 | 0.396 | -0.619 | 0.0490 |
| 3.937 | -2.094 | -1.063 | 0.387 | -0.676 | 0.0418 |
| 4.245 | -2.497 | -1.145 | 0.379 | -0.766 | 0.0362 |
| 4.552 | -2.923 | -1.172 | 0.369 | -0.803 | 0.0318 |
| 4.859 | -3.370 | -1.210 | 0.361 | -0.849 | 0.0281 |
| 5.166 | -3.839 | -1.258 | 0.352 | -0.906 | 0.0251 |
| 5.678 | -4.602 | -1.294 | 0.341 | -0.953 | 0.0212 |
| 6.021 | -5.179 | -1.304 | 0.327 | -0.977 | |
| 6.430 | -5.893 | -1.338 | 0.322 | -1.016 | |
| 7.659 | -7.834 | -1.466 | 0.303 | -1.163 | |
| 8.888 | -9.942 | -1.536 | 0.286 | -1.250 | |

Table 6. Continued

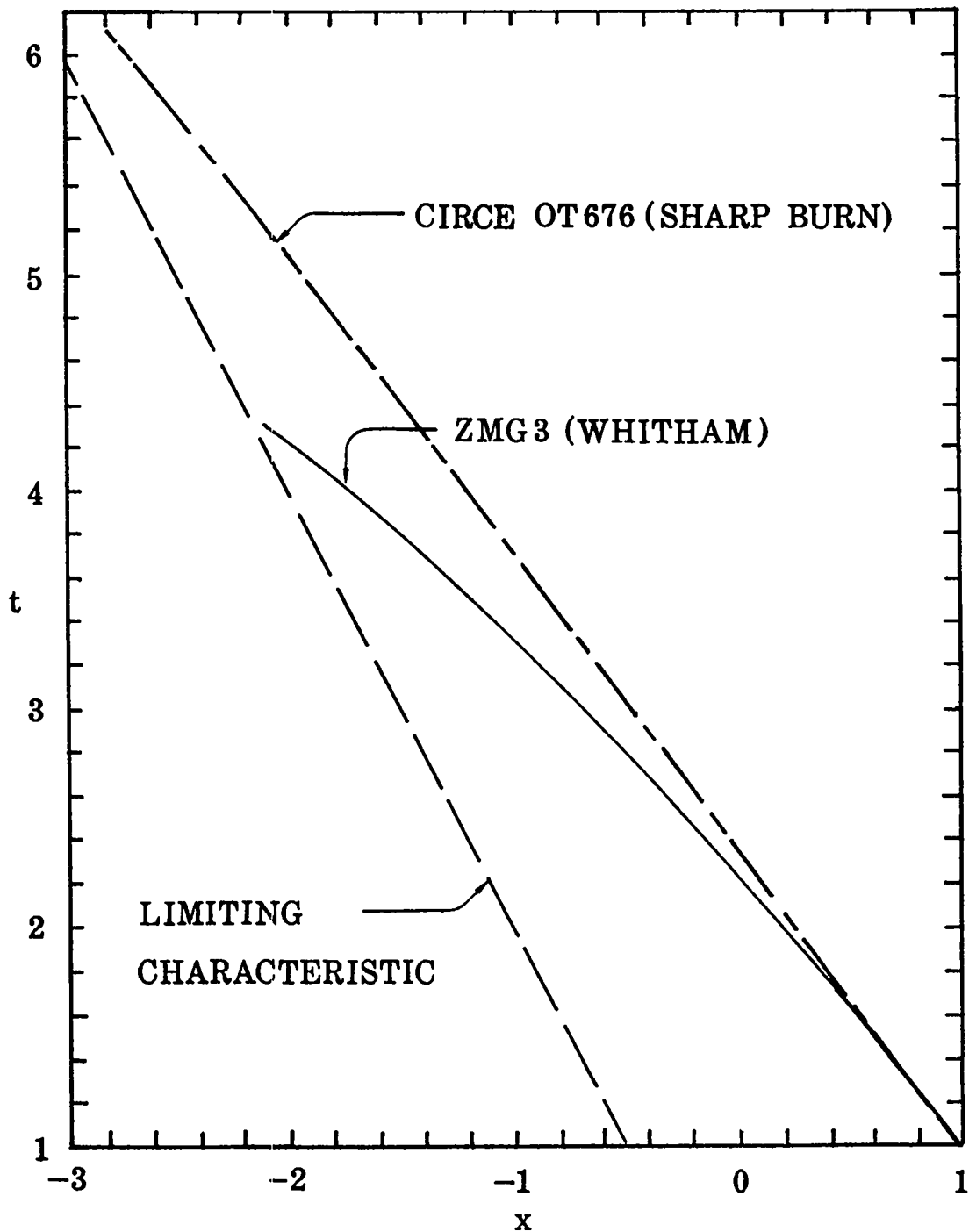| t | x | $u_s$ | $c_s$ | $dx/dt = u_s + c_s$ (behind shock) | $p_{wall}$ (megabars) |
|---|---|---|---|---|---|
| 9.297 | -10.585 | -1.526 | 0.282 | -1.244 | |
| 9.707 | -11.241 | -1.526 | 0.276 | -1.250 | |
| 10.117 | -11.903 | -1.538 | 0.269 | -1.269 | |
| 10.936 | -13.571 | -1.616 | 0.266 | -1.350 | |
| 11.755 | -14.944 | -1.609 | 0.258 | -1.351 | |
| 12.165 | -15.642 | -1.613 | 0.253 | -1.360 | |
| 12.574 | -16.345 | -1.622 | 0.249 | -1.373 | |
| 14.296 | -19.873 | -1.721 | 0.241 | -1.480 | |
| 15.934 | -22.809 | -1.715 | 0.231 | -1.484 | |
| 19.210 | -28.886 | -1.761 | 0.211 | -1.550 | |
| 20.849 | -31.958 | -1.787 | 0.205 | -1.582 | |
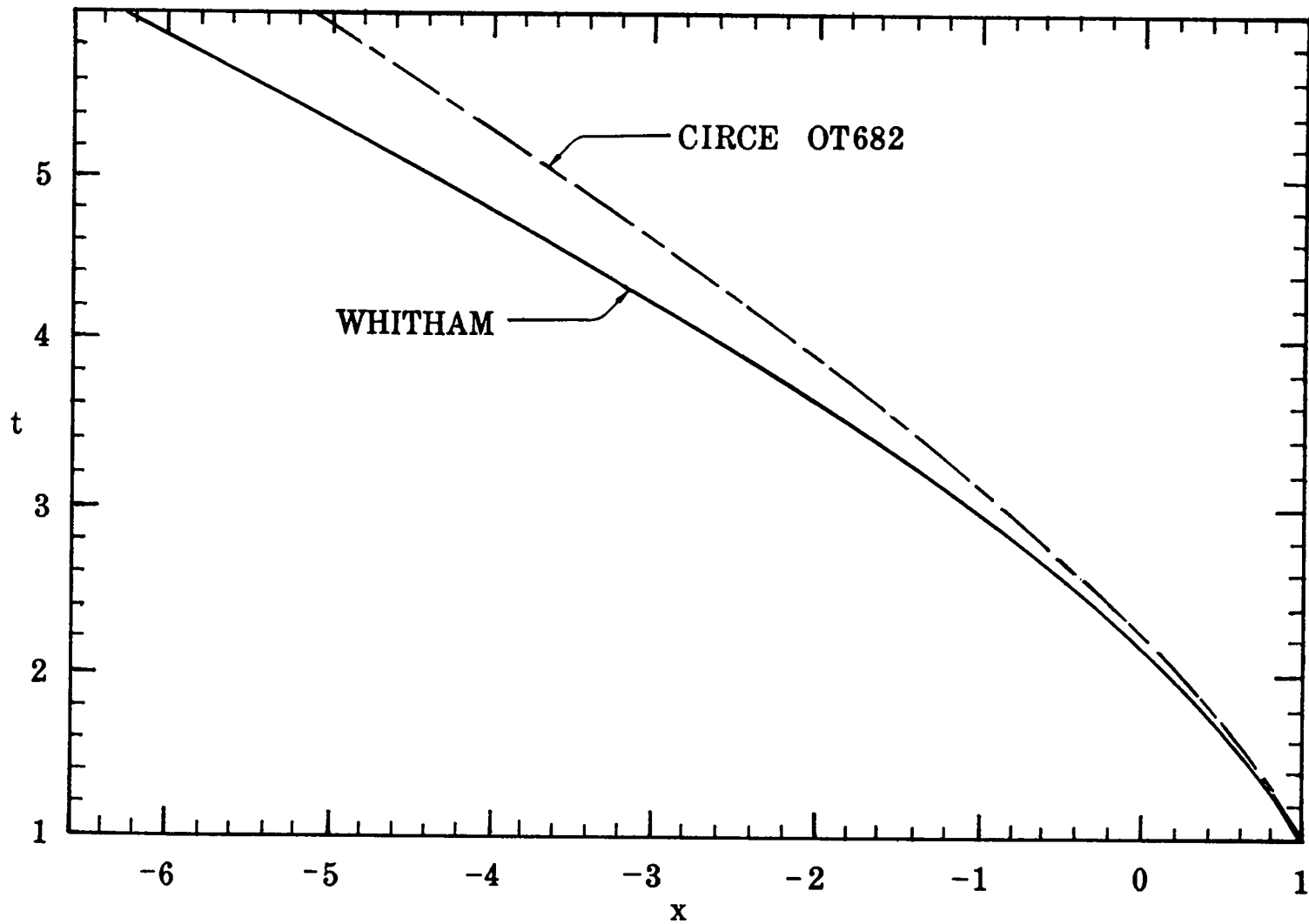
Figure 8. Reflected Shock Curves, Whitham Method and Circe $\gamma=1.4$

Table 7. Reflected Shock Data, Circe OT676, $\gamma = 3$, Sharp Detonation. [Note: $p^*_{wall}$ scaled to match Whitham results ($p_w \times 0.3725$)]

| t | x | $u_s$ | $c_s$ | $dx/dt = u_s + c_s$ (behind shock) | $p_{wall}$ (megabars) | $p^*_{wall}$ |
|---|---|---|---|---|---|---|
| 1.070 | 0.951 | -0.0117 | 0.926 | 0.914 | 0.488 | 1.818 |
| 1.173 | 0.873 | -0.102 | 0.918 | 0.816 | 0.369 | 1.375 |
| 1.275 | 0.788 | -0.138 | 0.809 | 0.671 | 0.288 | 1.073 |
| 1.480 | 0.635 | -0.210 | 0.679 | 0.469 | 0.185 | 0.689 |
| 1.685 | 0.487 | -0.287 | 0.622 | 0.335 | 0.125 | 0.466 |
| 1.889 | 0.336 | -0.331 | 0.556 | 0.225 | 0.0889 | 0.331 |
| 2.094 | 0.177 | -0.361 | 0.489 | 0.128 | 0.0653 | 0.243 |
| 2.229 | 0.027 | -0.393 | 0.446 | 0.053 | 0.0494 | 0.184 |
| 2.504 | -0.121 | -0.421 | 0.407 | -0.014 | 0.0382 | 0.142 |
| 2.709 | -0.282 | -0.451 | 0.406 | -0.045 | 0.0302 | 0.112 |
| 2.913 | -0.414 | -0.477 | 0.383 | -0.094 | 0.0243 | 0.0905 |
| 3.118 | -0.576 | -0.477 | 0.349 | -0.128 | 0.0198 | 0.0736 |
| 3.323 | -0.678 | -0.490 | 0.329 | -0.161 | 0.0164 | 0.0611 |
| 3.528 | -0.853 | -0.508 | 0.324 | -0.184 | 0.0137 | 0.0510 |
| 3.733 | -1.014 | -0.518 | 0.290 | -0.228 | 0.0116 | 0.0432 |
| 4.142 | -1.297 | -0.537 | 0.290 | -0.247 | 0.00846 | 0.0315 |
| 4.552 | -1.598 | -0.558 | 0.278 | -0.280 | 0.00637 | 0.0237 |
| 4.961 | -1.930 | -0.564 | 0.244 | -0.320 | 0.00492 | 0.0183 |
| 5.064 | -1.987 | -0.576 | 0.232 | -0.344 | 0.00463 | 0.0172 |
| 5.473 | -2.293 | -0.590 | 0.221 | -0.369 | | |

Table 7. Continued

| t | x | $u_s$ | $c_s$ | $dx/dt = u_s + c_s$ (behind shock) | $P_{wall}$ (megabars) | $P^*_{wall}$ |
|---|---|---|---|---|---|---|
| 5.883 | -2.546 | -0.596 | 0.215 | -0.381 | | |
| 5.985 | -2.692 | -0.605 | 0.208 | -0.397 | | |
| 6.088 | -2.756 | -0.615 | 0.250 | -0.365 | | |
| 6.190 | -2.821 | -0.609 | 0.241 | -0.368 | | |
| 6.293 | -2.888 | -0.608 | 0.229 | -0.379 | | |
| 6.395 | -2.957 | -0.610 | 0.215 | -0.395 | | |
| 6.497 | -3.026 | -0.616 | 0.207 | -0.409 | | |
| 6.600 | -3.096 | -0.623 | 0.189 | -0.434 | | |
| 6.804 | -3.236 | -0.637 | 0.171 | -0.466 | | |

Figure 9. Reflected Shock Curves, Whitham Method and Circe $\gamma=3.0$

Table 8.  Reflected Shock Data, Graphical Characteristic Solution, $\gamma = 3$.

| t | x | $u_s$ | $c_s$ | $dx/dt = u_s + c_s$ (behind shock) |
|---|---|---|---|---|
| 1.000 | 1.000 | 0.0 | 1.009 | 1.009 |
| 1.020 | 0.984 | -0.016 | 0.992 | 0.976 |
| 1.051 | 0.960 | -0.042 | 0.971 | 0.929 |
| 1.070 | 0.945 | -0.056 | 0.949 | 0.893 |
| 1.100 | 0.921 | -0.077 | 0.927 | 0.850 |
| 1.127 | 0.900 | -0.095 | 0.907 | 0.812 |
| 1.183 | 0.856 | -0.121 | 0.857 | 0.736 |
| 1.240 | 0.812 | -0.153 | 0.822 | 0.669 |
| 1.290 | 0.773 | -0.180 | 0.793 | 0.613 |
| 1.370 | 0.711 | -0.218 | 0.751 | 0.533 |
| 1.536 | 0.583 | -0.271 | 0.666 | 0.395 |
| 1.645 | 0.500 | -0.306 | 0.627 | 0.321 |
| 1.864 | 0.335 | | | |
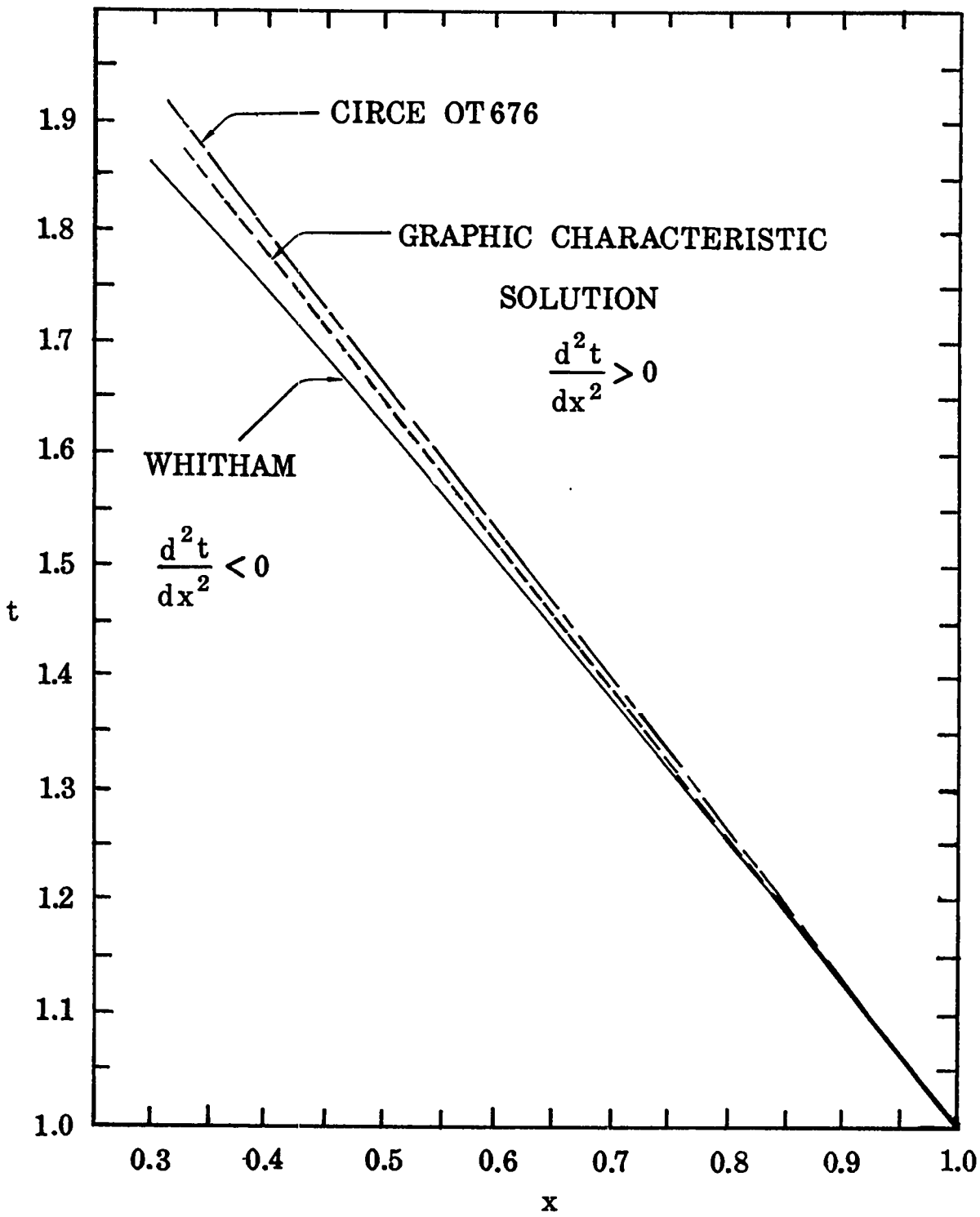
Figure 10. Reflected Shock Curves, $\gamma=3.0$, Comparison Between
Whitham Solution, Circe and Graphical Characteristic
Solution

The data of Tables 6 and 7 can be considered with regard to a discontinuity in the flow behind the shock for $\gamma > 2$ as discussed above. For $\gamma = 3.0$ there is a reversal in the trend of the characteristic direction behind the shock starting at $t = 6.088$; however, for $\gamma = 1.4$ there is also such a reversal at $t = 9.297$. It appears, upon further investigation of the numerical results, that the character of the numerical method does not make a definite conclusion possible since the flow behind the shock displays "secondary shocks" (defined by a non-vanishing pseudo-viscosity) even before the reversal in the trend of the characteristic direction noted above.

# APPENDIX I

Notation:  $d_i$; i = 0, 1, 2 - coefficients in quadratic expression for t [Equation (73)]

$d_3$ - defined as $d_0$-1

a, b - the coefficients of Equation (71)

$b_n$ = (1+nb), i.e., $b_1$ = 1+b, $b_2$ = 1+2b, etc.

## $\gamma = 1.4$

$P_7 = d_2 b_5/240(2+7b)$

$P_6 = [(5d_2 b_4 a + d_1 b_5) - 1680\ P_7\ ab_2]/240b_4$

$P_5 = [(10d_2 b_3 a^2 + 5d_1 b_4 a + d_3 b_5) - 1680\ a^2 P_7 - 480a P_6(2+5b)]/80b_5$

$P_2 = [(5b_1 a^4 d_3 + a^5 d_1) - 400a^4 b_1 P_5 - 480a^5(2+3b)P_6 - 1680a^6 b_2 P_7]/320a(b-2)$

$P_4 = [(d_2 a^5 + 5d_1 b_1 a^4 + 10d_3 b_2 a^3) - 1680a^5 b_6 P_7 - 1200a^4 b_4 P_6 - 800a^3 b_2 P_5$

$\qquad\qquad\qquad\qquad - 160(1-4b)P_2]/960a^2$

$P_0 = [d_3 a^5 - 480P_7 a^7 - 240P_6 a^6 - 80P_5 a^5 - 160P_2 a^2]/960$

$P_3$ arbitrary, set = 0

$P_1$ arbitrary, set = 0

To determine the $P_n$'s coefficients of like powers of $\xi$ in Equation (74) are equated to zero. $P_7 = P_7(a,b,d_i)$ is then determined by equating the coefficient of $\xi^7$ to zero and $P_n = P_n(P_{n+1}, \ldots, P_7, a,b,d_i)$ by setting the coefficient of $\xi^n$ to zero. This procedure breaks down for $P_3$ and $P_1$; these constants are indeterminate and found to be arbitrary. $P_2$ and $P_0$ are independent of $P_3$ and $P_1$. $P_4$ represented a special problem. For the case where only terms linear in b were retained $P_4$ could not be obtained from the coefficient of $\xi^4$; however, by taking the derivative of Equation (74) with respect to $\xi$, $P_2$ could be determined independently of $P_4$ and then the original expression for $P_2[P_2=P_2(P_4,P_5,P_6,P_7,a,b,d_i)]$ could be inverted and solved for $P_4$.

The case where terms of order $b^2$ were retained was again independent of $P_3$ and $P_1$. $P_4$ could be determined directly but the expression was very unstable numerically since changes of 2 percent in $P_5$, $P_6$, and $P_7$ resulted in changes of 150 percent in $P_4$. Because of this $P_4$ was evaluated in the same manner as used in the linear solution.

$\underline{\gamma = 3}$

$$P_5 = -0.5b_1d_4/(1+b^5)$$

$$P_4 = -[0.5(b_1d_3+ad_4) + 5ab^4P_5]/(1+b^4)$$

$$P_3 = -[0.5(b_1d_2+ad_3) + 10a^2b^3P_5 + 4ab^3P_4]/(1+b^3)$$

$$P_2 = -[0.5(b_1d_1+ad_2) + 10a^3b^2P_5 + 6a^2b^2P_4 + 3ab^2P_3]/(1+b^2)$$

$$P_1 = -[0.5(b_1d_5+ad_1) + 5a^4bP_5 + 4a^3bP_4 + 3a^2bP_3 + 2abP_2]/(1+b)$$

$$P_0 = -[0.5ad_5+a^5P_5+a^4P_4+a^3P_3+a^2P_2+aP_1]/2$$

These coefficients $P_n$ were obtained without complication by setting the coefficients of $\xi_n$ in Equation (85) to zero.

APPENDIX II

The purpose of this appendix is to demonstrate that a weak shock entering a centered rarefaction ending in a vacuum will, for $\gamma > 2$, generate a discontinuity behind the shock which propagates back into the fluid. This occurs when the shock reaches sufficient strength.

We shall begin by considering a strong shock in a centered rarefaction as sketched below.
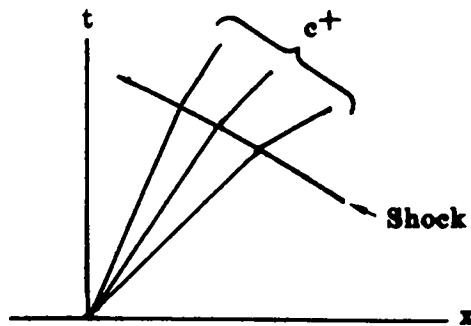


The $C^+$ characteristics can be represented as

Before the Shock: (a) $\dfrac{dx}{dt} = \dfrac{x}{t} = u + c = \eta$

(b) $\dfrac{u}{2} + \dfrac{c}{\gamma-1} = r(\eta)$         (A1)

After the Shock: $\dfrac{dx}{dt} = u_s + c_s = \emptyset.$         (A2)

We can also write down the strong shock relations (see for example ref.4, p.121-122)

$$u_s = \frac{2U}{\gamma+1} + \frac{\gamma-1}{\gamma+1} u \qquad \text{(A3)}$$

$$c_s = -\frac{\sqrt{2\gamma(\gamma-1)}}{\gamma+1} (U-u). \qquad \text{(A4)}$$

The shock velocity can be represented about $\eta_1$ by

$$U = U_0 + U_1(\eta-\eta_1) + U_2(\eta-\eta_1)^2 + \ldots \qquad \text{(A5)}$$

We also have for the centered rarefaction

$$\frac{u}{2} - \frac{c}{\gamma-1} = s_0, \text{ a constant.} \qquad \text{(A6)}$$

Combining (A1a) and (A6) one obtains

$$c = \frac{\gamma-1}{\gamma+1} (\eta-2s_0) \qquad \text{(A7)}$$

$$u = \frac{\gamma-1}{\gamma+1} (\frac{2\eta}{\gamma-1} + 2s_0). \qquad \text{(A8)}$$

And by introducing Equations (A7) and (A8) into (A1b) we have

$$r(\eta) = \frac{2}{\gamma+1} \eta + \frac{\gamma-3}{\gamma+1} s_0. \qquad \text{(A9)}$$

Substituting Equations (A3) and (A4) into (A2) and replacing u, c, and U in this expression by (A7), (A8), and (A5) (to first order terms) there results

$$\phi = \frac{2}{\gamma+1}[U_0 + U_1(\eta - \eta_1)] + (\frac{\gamma-1}{\gamma+1})^2(\frac{2\eta}{\gamma-1} + 2s_0)$$

$$-\sqrt{\frac{2\gamma(\gamma-1)}{\gamma+1}}\;[U_0 + U_1(\eta-\eta_1) - \frac{2\eta}{\gamma+1} - 2s_0\frac{\gamma-1}{\gamma+1}] \qquad\qquad (A10)$$

and

$$\frac{d\phi}{d\eta} = \frac{2}{\gamma+1}\left[U_1\left(1 - \sqrt{\frac{\gamma(\gamma-1)}{2}}\right) + \frac{2}{\gamma+1}\left(\frac{\gamma-1}{2} + \sqrt{\frac{\gamma(\gamma-1)}{2}}\right)\right]. \qquad (A11)$$

Looking at the coefficient of $U_1$ we find

$$\left(1 - \sqrt{\frac{\gamma(\gamma-1)}{2}}\right) < 0 \qquad\qquad \text{for } \gamma > 2$$

$$\left(1 - \sqrt{\frac{\gamma(\gamma-1)}{2}}\right) = 0 \qquad\qquad \text{for } \gamma = 2$$

$$\left(1 - \sqrt{\frac{\gamma(\gamma-1)}{2}}\right) > 0 \qquad\qquad \text{for } 1 < \gamma < 2$$

which means that the sign of $d\phi/d\eta$ depends both on $\gamma$ and the magnitude (and sign) of $U_1 = dU/d\eta_{\eta=\eta_1}$. Assuming $U_1 > 0$, it is then possible to have $d\phi/d\eta < 0$ for sufficiently large $U_1$. We shall now demonstrate that $U_1$ does indeed get very large at the tail of the rarefaction and

hence for $\gamma > 2$, $d\phi/d\eta < 0$ (note for $\gamma < 2$, $d\phi/d\eta > 0$ for all positive $U_1$).

Using the characteristic rule

$$dp_s - \rho_s c_s du_s = 0 \tag{A12}$$

and the strong shock relations

$$p_s = \frac{2}{\gamma+1} \rho(U-u)^2 \tag{A13}$$

$$\rho_s = \frac{\gamma+1}{\gamma-1} \rho \tag{A14}$$

along with those already introduced [Equations (A3) and (A4)] we have (since all variables are functions of $\eta$)

$$p_s' = \frac{4}{\gamma+1} \rho(U-u)(U'-u') + \frac{2}{\gamma+1}(U-u)^2 \rho'$$

$$u_s' = \frac{2}{\gamma+1} U' + \frac{\gamma-1}{\gamma+1} u'$$

(where primes denote differentiation with respect to $\eta$). Combining the above equations yields

$$\frac{4}{\gamma+1} \rho(U-u)(U'-u') + \frac{2}{\gamma+1}(U-u)^2\rho' + \sqrt{\frac{2\gamma}{\gamma-1}}\, \rho(U-u)\left[\frac{2}{\gamma+1}(U'-u')+u'\right] = 0. \tag{A15}$$

We note that in the simple wave region

$$\frac{\rho'}{\rho} = \frac{2}{\gamma-1}\left(\frac{1}{c}\right). \tag{A16}$$

Introducing Equations (A5), (A7), (A8), and (A16) into (A15) we obtain

$$2\left(U_1 - \frac{2}{\gamma+1}\right) + \frac{2(\gamma+1)}{(\gamma-1)^2}(\eta-2s_0)^{-1}\left[U_0+U_1(\eta-\eta_1) - \frac{2}{\gamma+1}\eta - \frac{2(\gamma-1)}{(\gamma+1)}s_0\right]$$

$$+\sqrt{\frac{2\gamma}{\gamma-1}}\left(U_1 - \frac{2}{\gamma+1} + 1\right) = 0.$$

Setting $\eta = \eta_1$ and solving for $U_1$ there results

$$U_1 = \frac{2}{\gamma+1}\left[2 - \sqrt{\frac{\gamma(\gamma-1)}{2}}\right] - \frac{2(\gamma+1)(U_0-u)}{(\gamma-1)^2(\eta_1-2s_0)}. \tag{A17}$$

Now on the limiting characteristic $c \to 0$ hence by Equation (A6), $u \to 2s_0$.
But $\eta = u + c$, therefore at limiting characteristic $\eta \to u \to 2s_0$.

Letting $\eta_1$ approach the limiting characteristic means the second
term on the right increases without bound. Since $(U_0-u) < 0$ we have

$$\text{as } \eta_1 \to 2s_0 \qquad U_1 \to \infty . \tag{A18}$$

Having considered the strong shock at the tail of the rarefaction
we shall now consider a weak shock at the head of a rarefaction. For
a weak shock we have the approximate relations (see for example ref.4,p.122),

$$u_s = u + \frac{4}{\gamma+1} [U-(u-c)]$$

$\qquad$ (A19)

$$c_s = c - 2\frac{\gamma-1}{\gamma+1} [U-(u-c)]$$

$\qquad$ (A20)

$$\frac{U-u}{c} + 1 = 0.$$

$\qquad$ (A21)

Combining Equations (A19) and (A20) with (A7) and (A8) and utilizing (A5) we have

$$u_s = \frac{\gamma-1}{\gamma+1}\left(\frac{2\eta}{\gamma-1} + 2s_0\right) + \frac{4}{\gamma+1}\left[U_0+U_1(\eta-\eta_1) - \frac{3-\gamma}{\gamma+1}\eta - 4\frac{\gamma-1}{\gamma+1}s_0\right]$$

$$c_s = \frac{\gamma-1}{\gamma+1}(\eta-2s_0) - 2\frac{\gamma-1}{\gamma+1}\left[U_0+U_1(\eta-\eta_1) - \frac{3-\gamma}{\gamma+1}\eta - 4\frac{\gamma-1}{\gamma+1}s_0\right]$$

which combined with Equation (A2) gives

$$\phi = \eta + 2(\frac{3-\gamma}{\gamma+1})\left[U_0+U_1(\eta-\eta_1) - \frac{3-\gamma}{\gamma+1}\eta - 4\frac{\gamma-1}{\gamma+1}s_0\right].$$

$\qquad$ (A22)

Differentiating Equation (A22) one obtains

$$\frac{d\phi}{d\eta} = 1 - 2\left(\frac{3-\gamma}{\gamma+1}\right)^2 + 2\left(\frac{3-\gamma}{\gamma+1}U_1\right).$$

$\qquad$ (A23)

Combining Equations (A5) and (A21) gives

$$U_0 + U_1(\eta-\eta_1) = u - c$$

66

which by Equations (A7) and (A8) is equivalent to

$$U_0 + U_1(\eta-\eta_1) = \frac{3-\gamma}{\gamma+1} \eta + 4\frac{\gamma-1}{\gamma+1} s_0.$$

Taking $d/d\eta$ we have

$$U_1 = \frac{3-\gamma}{\gamma+1} \tag{A24}$$

for a weak shock, which combined with Equation (A23) gives

$$\frac{d\phi}{d\eta} = 1 > 0. \tag{A25}$$

Summarizing, it has been shown that for a weak shock entering a rarefaction fan, $d\phi/d\eta > 0$. This shock will increase in strength as it propagates through the rarefaction. For a strong shock approaching the limiting characteristic it was also shown that $d\phi/d\eta > 0$ for $\gamma < 2$ and $d\phi/d\eta < 0$ for $\gamma > 2$, hence for $\gamma > 2$ there is a change of sign in $d\phi/d\eta$. This change in sign implies a discontinuity in the flow behind the shock (see sketch below).
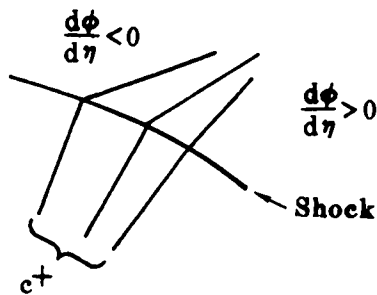
# APPENDIX III

This appendix illustrates the graphical procedure for computing the reflected shock curve and the flow between the shock and the wall (see for example ref.5).

The fundamental equations can be written as

Continuity
$$\frac{\partial \rho}{\partial t} + \frac{\partial (\rho u)}{\partial x} = 0 \qquad (B1)$$

Momentum
$$\frac{\partial u}{\partial t} + u \frac{\partial u}{\partial x} = -\frac{1}{\rho} \frac{\partial p}{\partial x} \qquad (B2)$$

Entropy condition
$$\frac{Ds}{Dt} = \frac{\partial s}{\partial t} + u \frac{\partial s}{\partial x} = 0 \qquad (B3)$$

Equation of State
    (a)  $p = \rho RT$

    (b)  $c^2 = \gamma p/\rho = \gamma RT$

    (c)  $s - s_1 = c_p \ell n \frac{T}{T_1} - R \ell n \frac{p}{p_1}$  (B4)

Combining Equations (B1), (B2), and (B4) one obtains

$$\frac{\partial}{\partial t}\left(\frac{2}{\gamma-1} \pm c\right) + (u \pm c)\frac{\partial}{\partial x}\left(\frac{2}{\gamma-1} c \pm u\right) = \frac{c}{R}\left(\frac{Ds}{Dt} \pm \frac{c}{\gamma}\frac{\partial s}{\partial x}\right) \qquad (B5)$$

68

where the left side is the derivative of $\frac{2}{\gamma-1} c \pm u$ in the direction $dx/dt = u \pm c$ in the x,t plane.

It is convenient to define the derivatives in the characteristic directions as

$$\frac{\delta^+}{\delta t} = \frac{\partial}{\partial t} + (u+c) \frac{\partial}{\partial x}$$

$$\frac{\delta^-}{\delta t} = \frac{\partial}{\partial t} + (u-c) \frac{\partial}{\partial x} \; . \tag{B6}$$

The Riemann variables are defined as

$$P = \frac{2}{\gamma-1} c + u$$

$$Q = \frac{2}{\gamma-1} c - u. \tag{B7}$$

Since $D/Dt = \partial/\partial t + u \, \partial/\partial x$ it is possible to eliminate the $ds/dx$ term in Equation (B5) as follows;

$$c \frac{\partial}{\partial x} = \frac{\delta^+}{\delta t} - \frac{D}{Dt} = - \frac{\delta^-}{\delta t} + \frac{D}{Dt}.$$

Noting that for the flow under considerations $Ds/Dt = 0$, Equations (B5) become

(a) $\quad \dfrac{\delta^+ P}{\delta t} = c \dfrac{\delta^+ s}{\delta t}$

(b) $\quad \dfrac{\delta^- Q}{\delta t} = c \dfrac{\delta^- s}{\delta t}$ $\hspace{4cm}$ (B8)

where velocities have been suitably normalized and the entropy has been normalized on $\gamma R$.

Summarizing, we now have

$$\dfrac{\delta^+ P}{\delta t} = c \dfrac{\delta^+ s}{\delta t} \qquad \text{on curves } \dfrac{dx}{dt} = u + c \hspace{2cm} \text{(B9)}$$

$$\dfrac{\delta^- Q}{\delta t} = c \dfrac{\delta^{..} s}{\delta t} \qquad \text{on curves } \dfrac{dx}{dt} = u - c \hspace{2cm} \text{(B10)}$$

$$\dfrac{Ds}{Dt} = 0 \qquad \text{on curves } \dfrac{dx}{dt} = u \, . \hspace{2cm} \text{(B11)}$$

For a finite difference approximation these equations can be replaced by equations of the form

$$\Delta^+ P_{12} = \bar{c}_{12} \, \Delta^+ s_{12} \hspace{4cm} \text{(B12)}$$

where $\Delta^+ P_{12}$ is the difference in P between points 1 and 2 on a particular $C^+$ characteristic. $\bar{c}_{12}$ is the average sound speed between 1 and 2 along the characteristic.

At shock points these equations do not hold but the Rankine-Hugoniot equations apply. If the unprimed quantities apply before the shock and

the primed quantities after the shock we have for a leftward running shock

$$\frac{Q'-Q}{c} = \frac{2}{\gamma-1} \left\{ \frac{1}{M} \left[ \left( 1 - \frac{2}{\gamma+1}(M^2-1) \right) \left( 1 + \frac{\gamma-1}{\gamma+1}(M^2-1) \right) \right]^{1/2} -1 \right\} + \frac{2}{\gamma+1} M \left( 1 - \frac{1}{M^2} \right)$$

(B13)

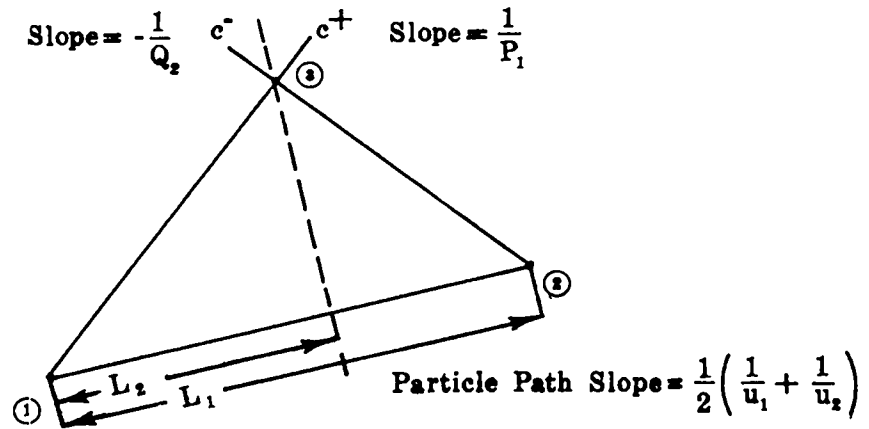$$\frac{u'-u}{c} = - \frac{2}{\gamma+1} M \left( 1 - \frac{1}{M^2} \right)$$

(B14)

$$\frac{c'}{c} = \frac{1}{M} \sqrt{ \left[ 1 + \frac{2\gamma}{\gamma+1}(M^2-1) \right] \left[ 1 + \frac{\gamma-1}{\gamma+1}(M^2-1) \right] }$$

(B15)

$$s' - s = \frac{1}{\gamma(\gamma-1)} \, \ell n \left[ 1 + \frac{2\gamma}{\gamma+1}(M^2-1) \right] + \frac{1}{\gamma-1} \ell n \, \frac{1}{M^2} \left[ 1 + \frac{\gamma-1}{\gamma+1}(M^2-1) \right] .$$

(B16)

It should be noted that the flow quantities in front of the shock are known.

For $\gamma = 3.0$ the following procedures were used for the various types of points. Iterations were not necessary in practice because of the slow changes in the variables.

## (A) Interior Point



All data are known at points 1 and 2, therefore
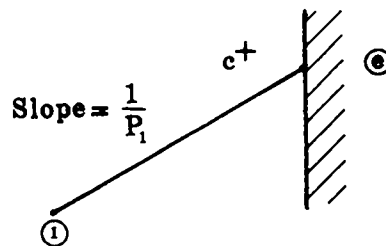
$$s_3 = \frac{L_2}{L_1}(s_2 - s_1) + s_1$$

$$P_3 = P_1 + c_1(s_3 - s_1)$$

$$Q_3 = Q_2 + c_2(s_3 - s_2)$$

$$u_3 = \frac{1}{2}(P_3 - Q_3)$$

$$c_3 = \frac{1}{2}(P_3 + Q_3)$$

## (B) Wall Point

All data are known at point 1, and $s_e$ is known from original shock reflection.
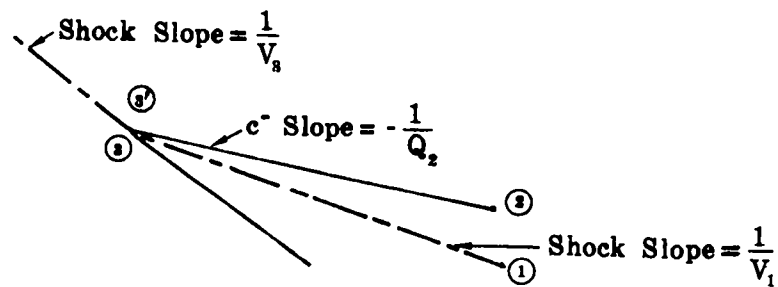
$$P_e = P_1 + (s_e - s_1)c_1$$

$$u_e = 0$$

$$c_e = P_e$$

$$Q_e = P_e$$

(C) Shock Point



All data are known at 3 (but not at 3') and 2.

Assume $\overline{Q}_3' = Q_2$, form $(\overline{Q}_3' - Q_3)/c_3$, and using Rankine-Hugoniot equation obtain $s_3'$.

Recompute $Q_3' = Q_2 + c_2(s_3' - s_2)$ and again form $(Q_3' - Q_3)/c_3$. Repeat until $Q_3'$ no longer changes, then from R-H equations one obtains $s_3'$, $c_3'$, $u_3'$, $M_3$. By definition $V_3 = u_3 - c_3 M_3$.

# REFERENCES

1.  G. B. Whitham, *On the Propagation of Shock Waves Through Regions of Non-Uniform Area or Flow*, Journal of Fluid Mechanics, Vol.4, Pt.4, p.337, August 1958.

2.  R. von Mises, *Mathematical Theory of Compressible Fluid Flow* (Academic Press, Inc., New York, 1958).

3.  Courant and Fredrichs, *Supersonic Flow and Shock Waves* (Interscience Publishers, Inc., New York, 1948).

4.  Oswatitsch and Kuerti, *Gas Dynamics* (Academic Press, Inc., New York, 1956).

5.  Rudinger, *Wave Diagrams for Non-steady Flow in Ducts* (D. Van Nostrand Company, Inc., New York, 1955).